TECHNICAL REPORT R-73

A STUDY OF THE SIMULATION OF FLOW WITH FREE-STREAM MACH NUMBER 1 IN A CHOKED WIND TUNNEL

By JOHN R. SPREITER, DONALD W. SMITH, and B. JEANNE HYETT

Ames Research Center
Moffett Field, Calif.

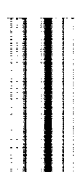

TECHNICAL REPORT R-73

A STUDY OF THE SIMULATION OF FLOW WITH FREE-STREAM MACH NUMBER 1 IN A CHOKED WIND TUNNEL

By JOHN R. SPREITER, DONALD W. SMITH, and B. JEANNE HYETT

SUMMARY

The degree to which experimental results obtained nder choking conditions in a wind tunnel with olid walls simulate those associated with an unounded flow with free-stream Mach number 1 is nvestigated for the cases of two-dimensional and xisymmetric flows. It is found that a close esemblance does indeed exist in the vicinity of the ody, and that the results obtained in this way are enerally at least as accurate as those obtained in a ransonic wind tunnel with partly open test section. ome of the results indicate, however, that substantial nterference effects, particularly those of the wave eflection type, may be encountered under certain onditions, both in choked wind tunnels and in ransonic wind tunnels, and that the reduction of hese interference effects to acceptable limits may equire the use of models of unusually small size.

INTRODUCTION

It was long believed that the phenomenon of hoking prevented the use of a closed wind tunnel o obtain data representative of unbounded flow ith free-stream Mach number 1, and that the esults obtained under choking conditions, although readily repeatable, were of no general ractical importance. A series of theoretical nvestigations, many of which are summarized by luderley in reference 1, has indicated, however, hat the flow in the vicinity of the model under hoking conditions has a close resemblance to an nbounded flow with free-stream Mach number 1, rovided the dimensions of the model are sufficiently small compared with those of the test sec-on. Although the important question of the magitude of the deviation has been examined for only very small number of two-dimensional flows past simple airfoils, principally wedges and flat plates, it is found in each case that the influence of the wall is relatively small for model sizes typical of standard wind-tunnel practice. The results of these investigations represent an important contribution to the knowledge of nonlinear wind-tunnel interference effects, and provide a strong indication, previously unsuspected, that measurements in a choked wind tunnel may be very useful in the study of transonic flows with free-stream Mach number 1.

Although some of the theoretical investigations of the flow in a choked wind tunnel date back about ten years, very little attention has been given to the actual use of a solid-wall wind tunnel to simulate flows with free-stream Mach number 1. This fact, together with a growing realization that experimental results obtained in transonic wind tunnels with partially open walls are sometimes subject to interference effects of large and unknown magnitude (see, e.g., refs. 2, 3, and 4), has prompted the present investigation. The purpose of the investigation is fourfold: first, to provide an experimental check on some of the quantitative theoretical results for simple two-dimensional airfoils; second, to provide information for additional cases, both two-dimensional and axisymmetric, for which the theoretical studies yield only a qualitative estimate of the interference effects; third, to provide additional information on interference effects at Mach number 1 in transonic wind tunnels with partially open walls; and fourth, to extend further the evaluation of results of recent theoretical developments that enable the calculation of pressure distributions for a wide variety of wings and bodies with free-stream Mach number 1. The accomplishment of this multiple

purpose is sought by following a consistent procedure in which experimental results obtained in a choked solid-wall wind tunnel are systematically compared with the corresponding results indicated both by conventional tests in transonic wind tunnels and by transonic flow theory. Existing theoretical and experimental results are used whenever available, but many of the results for the choked wind tunnel, as well as some of the other experimental and theoretical results, are new and were obtained specifically to complete certain aspects of the investigation.

QUALITATIVE DESCRIPTION OF FLOW

A qualitative understanding of several important features of flow in a choked wind tunnel, and the relation between them and the corresponding features of an unbounded flow with free-stream Mach number 1, can be had by considering the pair of diagrams shown in figure 1. Both diagrams show the conditions associated with a simple nonlifting body in either two-dimensional or axisymmetric flow. The aft part of the body has been omitted not only because most features of flow at Mach number 1 do not depend on the shape of this part of the body, but also to avoid discussion of complicating features associated with shock waves and, in the case of axisymmetric flow, with details of the model support system and with an imbedded region of subsonic flow that occurs near the rear tip of a complete body.

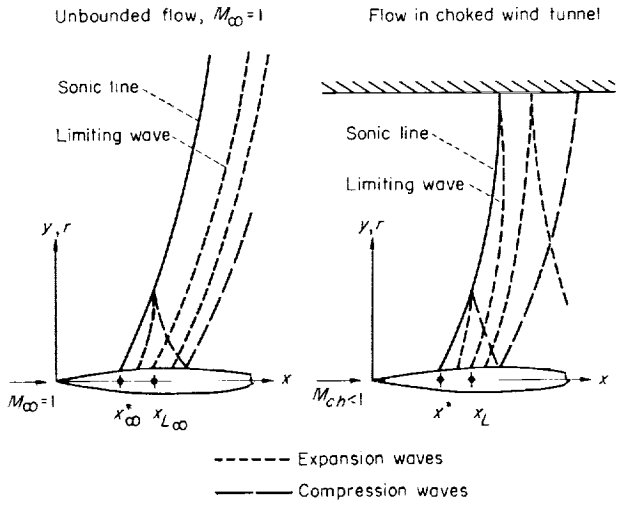

FIGURE 1. Sketches illustrating the principal features of the flow field in an unbounded stream and in a choked wind tunnel.

Consider first the diagram on the left representing unbounded flow with free-stream Mach number 1. Most of the features of this flow that are important here are associated with the sonic line which extends from the sonic point x_∞^* on the body to infinity and divides the regions of subsonic and supersonic flow. The flow is supersonic downstream of the sonic line and is characterized by a system of Mach waves which originate at the surface of the body and propagate outward into the fluid. Those that originate from points close behind the sonic point are expansion waves and curve so as to intersect the sonic line from which they reflect as compression waves. These, in turn, propagate through the fluid and, if the body is sufficiently long, strike the body and reflect as compression waves. Waves that originate from points farther from the sonic point intersect the sonic line farther from the body. Finally, there is a limiting wave, which originates from a point on the body designated x_{L_∞}, which must be situated downstream of the sonic point but upstream of the point of maximum thickness and that fails to meet the sonic lines even at infinitely great distances from the body. Inasmuch as the waves that originate from points on the body aft of x_{L_∞} can not have any effect on the subsonic region unless they coalesce to form a shock wave that extends to the sonic line, it follows that the shape of the part of the body situated downstream of x_{L_∞} can be varied within wide limits without producing any upstream effect on the flow. It may be noted that this restriction is overlooked in most discussions of the significance of the limiting wave, and that some erroneous conclusions have appeared in the literature (see, in particular, ref. 5) as a consequence.

Consider next the diagram on the right representing flow past the same body in a choked wind tunnel. As is well known, the Mach number of the flow far upstream of the model has a definite value less than unity for any given combination of model and test section. This quantity, designated the choking Mach number M_{ch}, is not of great importance in a discussion of flow in a choked wind tunnel, however, and it is more rewarding to concentrate on the properties of the part of the flow field situated in the general vicinity of the body. As in the case of the unbounded flow, there is a sonic line which extends from the

sonic point x^* on the body to the wall and separates the regions of subsonic and supersonic flow. There is also a limiting wave which extends from a point on the body designated x_L to the point of intersection of the sonic line and the wind-tunnel wall, and divides the waves from the body into two families according to whether or not they reach the sonic line and can hence influence the subsonic region upstream. Those that originate upstream of x_L reach the sonic line and reflect as illustrated in much the same manner as in the case of unbounded flow. Those that originate downstream of x_L do not propagate outward indefinitely as in the case of an unbounded flow, however, but reflect from the solid wall of the wind tunnel with unchanged sign. These waves lead, if the body is sufficiently long, to interference effects on the rear of the body that are of the wave-reflection type familiar from corresponding studies of interference effects in supersonic wind tunnels. It is evident, however, that there may be a region of substantial size that is free of such wave reflections and within which the flow in a choked wind tunnel bears at least a qualitative resemblance to an unbounded flow with free-stream Mach number 1. It is equally evident from a similar comparison that the flow in a choked wind tunnel is distinctly different from an unbounded flow with M_∞ equal to M_{ch}, except in the limit as the tunnel size increases to infinity relative to the model and M_{ch} approaches unity.

Several factors that affect the degree to which flow in a choked wind tunnel simulates unbounded flow with free-stream Mach number 1 can be examined on the basis of the foregoing discussion without resort to a complete quantitative analysis of the two flows. The most obvious, of course, is that the degree of simulation improves for a given body as the size of the test section is increased. It is equally evident, but perhaps more surprising, result is that the wave-reflection type of interference on the rear of the body is more likely to be a problem in tests of a thin body than of a thick body of the same length in a given test section. The reason is that the local Mach numbers remain nearer unity and hence the sonic line and Mach waves are more nearly normal to the flow direction for the thin body than for the thick body. It can also be seen from similar considerations that wave reflection is more likely to be a problem in tests of a body with maximum thickness far forward than with maximum thickness far aft.

It should be remarked that many of the interference effects described above also occur in the study of flows with free-stream Mach number 1 in a transonic wind tunnel with partly open walls. The principal differences are that choking does not occur in a transonic wind tunnel, and that the wave-reflection properties of the partly open walls may be of either sign and are much more complicated than those of solid walls. The latter factor may lead to a reduction in interference effects in a wind tunnel with partly open walls but does not necessarily do so, as is evidenced by the result given by Marschner in reference 6 that interference effects on a double-wedge airfoil, the only case for which complete theoretical information is available, are somewhat more than 10 percent greater in a wind tunnel with a completely open test section (i.e., a sonic free jet) than in a choked solid-wall wind tunnel. The transonic wind tunnel has the big advantage, however, of being capable of providing data not only for Mach number 1 but for all Mach numbers throughout the transonic range.

TWO-DIMENSIONAL FLOW

The case of two-dimensional flow is considered first because of the greater simplicity and completeness of the theoretical and experimental results.

SUMMARY OF PRINCIPAL THEORETICAL RESULTS

Consider two-dimensional flow of an inviscid compressible fluid past a thin airfoil of maximum thickness t and chord c placed as shown in figure 2 on the center line of a solid-wall wind tunnel operating in the choked condition. Consider

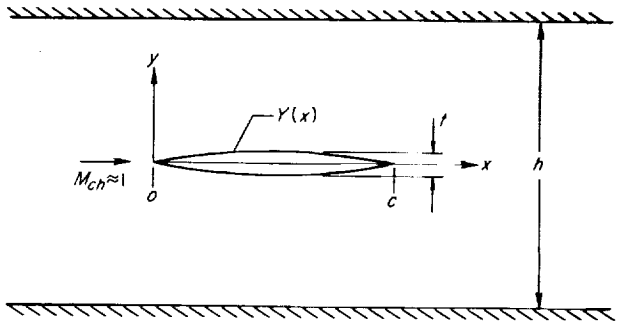

FIGURE 2.—View of airfoil, coordinate system, and principal dimensions.

further that the height h of the test section is sufficiently great that the choking Mach number is near unity. It is advantageous, for such a class of flows, to develop the solution in terms of deviations or perturbations from conditions associated with a uniform flow with sonic velocity a^* rather than in terms of perturbations from conditions associated with the uniform flow that occurs far upstream in the test section. The retention of only the leading terms in such a development leads immediately to the nonlinear equations of the small disturbance theory of nearly sonic flow (see, e.g., ref. 1). The principal equations of this theory are summarized below in terms of a Cartesian coordinate system oriented in such a way that the positive x axis extends in the downstream direction along the center line of the wind tunnel.

Basic equations.—Let U and V represent the components of the velocity parallel to the x and y axes, and define the perturbation velocity components u and v in such a way that $U=a^*+u$ and $V=v$. The quantities u and v can be expressed in terms of the gradient of a perturbation potential φ (i.e., $u=\varphi_x$, $v=\varphi_y$) that satisfies the following nonlinear partial differential equation:

$$\varphi_{yy}=\frac{\gamma+1}{a^*}\varphi_x\varphi_{xx} \tag{1}$$

where γ is the ratio of specific heats ($\gamma=1.4$ for air). The boundary conditions require that the flow be tangential to the wind-tunnel wall and the airfoil surface, and be of uniform velocity compatible with the choking Mach number infinitely far upstream of the model. The first condition requires that

$$(\varphi_y)_{y=h/2}=0 \tag{2}$$

The second and third conditions are approximated by

$$(\varphi_y)_{y=0}=a^*(dY/dx) \tag{3}$$

and

$$(\varphi_x)_{x=-\infty}=U_{ch}-a^*=-\frac{2a_{ch}^2}{\gamma+1}\left(\frac{1-M_{ch}^2}{U_{ch}+a^*}\right)\approx -\frac{2a^*}{\gamma+1}(1-M_{ch}) \tag{4}$$

where $Y(x)$ refers to the ordinates of the airfoil surface, and a_{ch} and U_{ch} refer to the speed of sound and velocity infinitely far upstream of the model. The pressure p is a quantity of prime interest and two different pressure coefficients are of interest i the following discussion. One is the usual co efficient $C_p=(p-p_{ch})/q_{ch}$ in which p_{ch} and q_{ch} refe to the values of the static and dynamic pressure that occur infinitely far upstream of the airfoi Another coefficient that is more useful in th discussion of flow in a choked wind tunnel i $C_p{}^*=(p-p^*)/q^*$ in which p^* and q^* refer to th theoretical values of the static and dynami pressures associated with flow at sonic velocity that is, $p^*=0.5283\ p_t$ and $q^*=0.3698\ p_t$ where t refers to the stagnation or total pressure. Th expressions that relate these pressure coefficient and the velocity are approximated in a manne consistent with the simplifications introduced i the differential equations and boundary condition thus

$$C_p{}^*=-\frac{2\varphi_x}{a^*},\quad C_p=-\frac{2[\varphi_x-(\varphi_x)_{x=-\infty}]}{a^*} \tag{5}$$

Similarity rule.—The equations enumerate above contain a similarity rule that relates th aerodynamic properties experienced by families c airfoils of affinely related geometry in choked win tunnels of arbitrary size. The ordinates of a members of such a family of airfoils are given b $Y/c=\tau f(x/c)$ where the thickness ratio τ must l small but is otherwise arbitrary, and the thickne distribution function $f(x/c)$ must be the same fo all members of the family. The similarity ru states that the pressures on the airfoils of th family are related in such a way that the followin functional dependence holds:

$$C_p{}^*/\tau^{2/3}=\mathrm{P}(H\tau^{1/3},x/c) \tag{6}$$

where H refers to the ratio h/c of the tunnel heigh to the airfoil chord. The influence of variatio of γ from case to case can easily be included i this and all of the relations that follow, but ha been omitted in order to take advantage of slight gain in simplicity that results from the fac that γ effectively disappears as a parameter sinc it has a constant value of 1.4 in nearly all con ventional transonic testing in which the workin fluid is air at ordinary temperatures and pressure The similarity rule also indicates the followin functional relation for the choking Mach numbe

$$(1-M_{ch})/\tau^{2/3}=\mathrm{M}(H\tau^{1/3}) \tag{7}$$

Simple considerations of similarity provid knowledge of the pertinent parameters, bu

cannot provide any information on the relations between the parameters. It is possible, however, to gain further insight into the interference effects in the region upstream of that influenced by wave reflection, without accepting the difficulties of solving particular examples in all detail, by considering the asymptotic behavior of the flow at great distances from an airfoil. Guderley has examined this aspect of the present problem in references 1 and 7, and has shown for a general two-dimensional airfoil in a choked wind tunnel that the deviation of the values for C_p^* from the corresponding values $(C_p^*)_{M_\infty=1}$ for the same airfoil in an unbounded flow with free-stream Mach number 1 is proportional to $(1-M_{ch})^3$ and inversely proportional to $(h/c')^{6/5}$ where c' is some length characteristic of the airfoil chord. Combination of this result and the similarity rule leads to the following pair of relations for C_p^* and M_{ch} for a family of affinely related airfoils:

$$\frac{\Delta C_p^*}{\tau^{2/3}}=\frac{C_p^*-(C_p^*)_{M_\infty=1}}{\tau^{2/3}}=\frac{\mathrm{P}(x/c)}{(H\tau^{1/3})^{6/5}} \tag{8}$$

$$\frac{1-M_{ch}}{\tau^{2/3}}=\frac{\mathrm{Const}}{(H\tau^{1/3})^{2/5}} \tag{9}$$

Certain statements regarding the conditions under which a choked wind tunnel is useful for the simulation of an unbounded two-dimensional flow with free-stream Mach number 1 can be made directly upon examination of equations (8) and (9). One observes first that the interference effects on the pressure distribution, as signified by the values for ΔC_p^*, are inversely proportional to the 6/5 power of the height-chord ratio H so that smaller errors result when smaller models are tested, as is certainly to be expected. Similarly, ΔC_p^* is proportional to $\tau^{4/15}$ so that the magnitude of the interference effects is smaller for thin airfoils than for thick airfoils. The quantity $(C_p^*)_{M_\infty=1}$ that is intended to be simulated is proportional to $\tau^{2/3}$, however, and the result emerges that the relative error $\Delta C_p^*/(C_p^*)_{M_\infty=1}$ is inversely proportional to $\tau^{2/5}$, and is hence larger for thin airfoils than for thick airfoils just as is found to be the case for the wave-reflection type of interference. These equations also indicate that the quantity $1-M_{ch}$ depends on a different combination of H and τ than does $\Delta C_p^*/(C_p^*)_{M_\infty=1}$, from which it follows that the quality of the simulation cannot be judged with certainty by the nearness to unity of the choking Mach number.

Although the fact that the ratio c'/c is a single constant for all members of a family of affinely related airfoils makes it permissible to drop the distinction between c' and c in writing equations (8) and (9), it should be recognized that the chord and maximum thickness of the airfoil are not the significant lengths associated with wind-tunnel interference at Mach number 1. The reason is that it is not the dimensions of the complete airfoil that appear in the asymptotic solution for the flow at great distances from the airfoil, but the dimensions of the part of the airfoil that can influence the subsonic part of the flow field. This point has been discussed by Barish in reference 8, who suggests the use of the dimensions of that part of the airfoil forward of the sonic point, even though it is evident that a somewhat greater part of the airfoil is actually of significance. This suggestion, which is based upon observations of the results of numerical calculations of the asymptotic flow fields of wedges and certain cusp-nosed airfoils, leads to the following expressions alternative to equations (8) and (9):

$$\frac{\Delta C_p^*}{\tau^{*2/3}}=\frac{\mathrm{P}\,(x/c^*)}{(H^*\tau^{*1/3})^{6/5}} \tag{10}$$

$$\frac{1-M_{ch}}{\tau^{*2/3}}=\frac{Const}{(H^*\tau^{*1/3})^{2/5}} \tag{11}$$

in which the quantities H^* and τ^* represent h/c^* and t^*/c^*, and t^* and c^* refer to the thickness and chord of the part of the airfoil forward of the sonic point. Inasmuch as the two sets of functional relations for C_p^* and M_{ch} are equivalent for a family of affinely related airfoils, the principal advantage of the latter formulation is that the function $\mathrm{P}(x/c^*)$ and the constant may be expected to be more nearly invariable for airfoils that are not affinely related. An example illustrating that parameters defined in this way are also of significance in the correlation of data from transonic wind tunnels having partly open walls has been given previously in reference 9. This example is of particular interest here because it confirms the result suggested by the above considerations that interference effects at Mach number 1 on a family of nonaffinely related smooth airfoils of given chord and thickness

increase as the point of maximum thickness is moved rearward across the chord. It should be noted that this trend is opposite to that described in the preceding section for interference effects of the wave reflection types.

Application to unbounded flow with free-stream Mach number 1. The foregoing relations for the flow in a choked wind tunnel reduce smoothly and continuously to the appropriate forms for unbounded flow with free-stream Mach number 1 as the height h of the test section increases to infinity, and the parameter $H\tau^{1/3}$ grows beyond all bounds for an airfoil of given geometry. This conclusion follows from the fact that ΔC_p^* and $1-M_{ch}$ are indicated by equations (8) and (9) to vanish as $H\tau^{1/3}$ approaches infinity. It follows further, assuming only that C_p^* is finite and different from zero, that the quantity $H\tau^{1/3}$ disappears as a parameter in equation (6) and that $C_p^*/\tau^{2/3}$ is a function only of x/c and airfoil thickness distribution function $f(x/c)$ for unbounded flow with free-stream Mach number 1. The latter result is, of course, the well-known transonic similarity rule described by von Kármán in reference 10.

The theoretical analysis of unbounded flow is fundamentally simpler than the analysis of flow in the bounded channel of a wind tunnel, and a number of methods, both approximate and exact, are now available for the calculation of the pressure distribution on a wide variety of airfoils in an unbounded flow with free-stream Mach number 1. Although these results will be drawn upon freely in the course of the following discussion, it would greatly exceed the scope and purpose of the present summary of theoretical results to attempt to review these investigations. This body of information has been reviewed recently in references 1 and 3, however, and the reader is referred to these sources for further information.

Numerical results for interference effects on wedge airfoils.—The function $P(x/c)$ and the constant that appear in equations (8) and (9) depend on the shape of the airfoil and are known at the present time for only wedge and flat-plate airfoils. Marschner has considered the case of a nonlifting double-wedge airfoil in reference 6 and has determined the following expressions for ΔC_p^* and M_{ch}:

$$\frac{\Delta C_p^*}{\tau^{2/3}}=\frac{1.802F(x/c)}{(H\tau^{1/3})^{6/5}} \tag{12}$$

$$\frac{1-M_{ch}}{\tau^{2/3}}=\frac{1.127}{(H\tau^{1/3})^{2/5}} \tag{13}$$

The function $F(x/c)$ varies as shown in figure 3 from a value of about ¼ near the leading and trailing edges to zero at the shoulder where the local velocity is sonic regardless of the relative dimensions of the airfoil and the test section.[1]

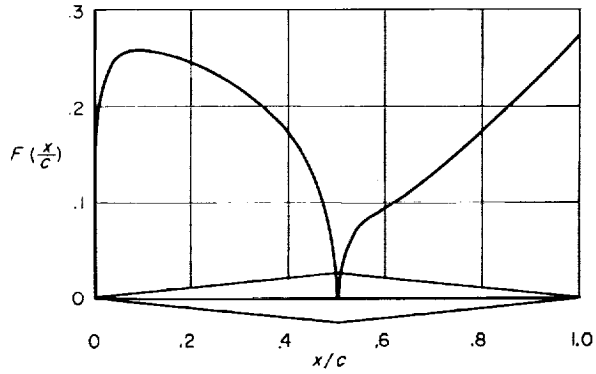

FIGURE 3.—Theoretical values for the function $F(x/c)$ in equation (12) for a symmetrical double-wedge airfoil (refs. 1 and 6).

The significance of the interference effects indicated by equation (12) can be judged by comparison with the values for $C_p^*/\tau^{2/3}$ on the same airfoil in an unbounded flow with free-stream Mach number 1 given in reference 11 by Guderley and Yoshihara and reproduced here in figure 4. An independent theoretical confirmation of these results is provided by several relaxation solutions given by Morioka in reference 12 for the special cases in which the height of the test section is such that the parameter $H\tau^{1/3}$ takes on the values ∞, 4.3, 2.27, and 1.44. It may be noted that the corresponding values for the height-chord ratios H associated with a 10-percent-thick airfoil are ∞, 9.3, 4.9, and 3.1. It is found that the corresponding values for the transonic similarity parameter, which Morioka writes as $\xi_\infty=(\gamma+1)^{1/3}(U_{ch}-a^*)/a^*\tau^{2/3}$ but which corresponds to $2(M_{ch}-1)/[(\gamma+1)\tau]^{2/3}$ if the approximate relation of equation (4) is introduced, are 0, −0.703, −0.921, and −1.116. These results lead to values for the choking Mach number of 1, 0.869, 0.829, and 0.795 if the first form of the parameter is used and to values of 1, 0.864, 0.822, and 0.784 if the second form is used.

[1] Attention of those who refer to reference 1 for a summary of the above analysis is called to the fact that the ordinates of the plot of the function F given in Abb. 100 should be diminished by a factor of 10.

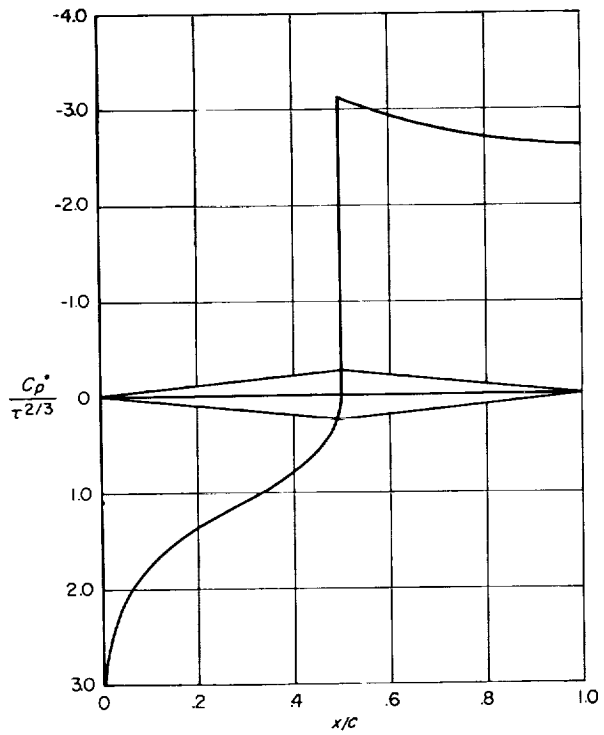

FIGURE 4.—Theoretical pressure distribution on a symmetrical double-wedge airfoil in an unbounded flow with free-stream Mach number 1 (refs. 1 and 11).

It is informative to compare the latter set of results with those indicated by equation (13), namely, 1, 0.864, 0.825, and 0.791. It can be seen that the results for the largest choking Mach number less than 1, and therefore for the largest finite height-chord ratio, agree perfectly, but that small deviations of increasing magnitude are apparent as the height-chord ratio and the choking Mach number are diminished. Such a trend is entirely consistent with the expected properties of the two sets of results because Marschner's analysis is based on the assumption that $H\tau^{1/3}$ is sufficiently large that only the leading terms need be retained, whereas this approximation is not introduced in the relaxation solutions of Morioka. The differences between the two sets of results are thus of particular interest because they provide a measure of the importance of the contribution of the higher order terms omitted in the analysis of Marschner. It must, of course, be assumed in making this statement that the relaxation calculations of Morioka are sufficiently accurate that differences of this magnitude are actually significant.

548698—60——2

The corresponding results for a lifting flat plate in a choked wind tunnel have been given by Guderley in references 13 and 1. Although the expression for $P(x/c)$ and the value for the constant that appear in equations (8) and (9) are naturally different from those indicated above for the nonlifting double-wedge airfoil, it is found that the numerical values are of about the same magnitude when the thickness ratio τ is replaced by the angle of attack in radians.

Additional results, approximate by Kusukawa (ref. 14) and exact by Helliwell (ref. 15), are also available for the case of free-streamline flow past a single-wedge airfoil. It is found that the numerical values for ΔC_p^* for a given value for M_{ch} agree well with those determined by Marschner for the front wedge, but that the relation between M_{ch} and $H\tau^{1/3}$ is much different for free-streamline flows than for flows such as considered by Marschner, Morioka, and Guderley in which acceleration to supersonic velocities through a Prandtl-Meyer expansion occurs at a convex corner. This difference extends not only to the constant, but also to the functional form of the relation in that the exponent 2/5 that appears in equation (9) is replaced by 2/3 in the free-streamline solution of Helliwell. The difference is to be anticipated as a consequence of the fact that the choking Mach number in free-streamline flow depends on the ultimate width of the wake, which is considerably greater than the maximum thickness of the airfoil, and is associated with a corresponding difference between the asymptotic solutions for the flows at great distances from the airfoil. It is appropriate to remark before closing this discussion that two other values for this exponent, namely, 2/7 and 1/2, are indicated by the approximate solutions of Kusukawa for free-streamline flow, and Helliwell for unseparated flow. The former theory is based on the use of Imai's WKB approximation (see ref. 16 for a résumé), and the latter on introduction of an assumption used previously by Cole (ref. 17) and also by Weinstein in reference 18 (see ref. 19 for a commentary), that the sonic line extending from the shoulder of the wedge is straight and normal to the flow at infinity upstream. All of the theories yield very nearly the same results for the values for C_p^* on the surface of the wedge at a given value of M_{ch}, however.

Numerical results for conditions along the wall.—Further insight into the nature of flow in a choked wind tunnel can be gained by consideration of the pressure or local Mach number distribution along the wall of the test section. The pertinent results from two independent investigations are summarized in figure 5. The line represents

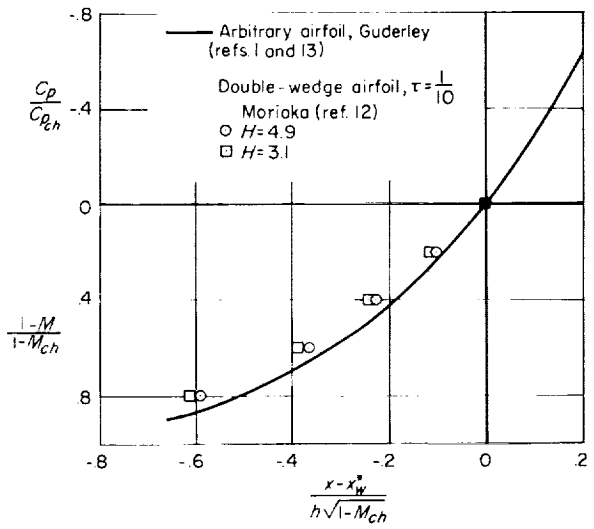

FIGURE 5.—Pressure and local Mach number distributions along the wall of the test section of a choked wind tunnel.

the values for either $C_p^*/C_{p_{ch}}^*$ or $(1-M)/(1-M_{ch})$ indicated by the theoretical investigations of Guderley reported in references 20 and 1.[2] It is applicable to any thin airfoil in a large wind tunnel operating in the choked condition. It should be noted, however, that the theory does not provide any correspondingly general relationship for the values for M_{ch} or $C_{p_{ch}}$ associated with an arbitrary airfoil, nor any information regarding the location with respect to the airfoil of the station along the wall x_w^* at which sonic velocity occurs.

The symbols represent the values indicated by the relaxation solutions of Morioka (ref. 12) for the conditions along the wall of a choked test section for the special case of a 10-percent-thick double-wedge airfoil. Two sets of results are shown. One represents the conditions associated with a test section having such dimensions that the height-chord ratio H is 4.9, the other that H is 3.1.

[2] Attention of those who refer to either of these references for further details is called to the fact that the abscissas of the plots corresponding to figure 5 should be increased by a factor of 10.

The approximate relation of equation (4) has been used in the calculation of the choking Mach number, and the resulting values for the two cases are 0.822 and 0.784 as noted in the preceding section. The results are thus comparable with the analytic results of Guderley except, once again, for the consequences of the fact that only the leading terms for large $H\tau^{1/3}$ are retained in the latter analysis. It can be seen that the general trends indicated by the two theories are qualitatively similar, but that quantitative differences of a systematic nature exist among the three sets of results. It can be seen, in particular, that the numerical results of Morioka for the large wind tunnel agree closer with the analytic results of Guderley than do the numerical results for the smaller wind tunnel. This trend is very similar to that indicated for the choking Mach number in the preceding section, and it is entirely consistent with the expected properties of the two theories.

The results of Morioka not only essentially confirm but supplement the more general, but less detailed, results of Guderley since the relaxation method provides complete information on conditions throughout the part of the field in which the flow is subsonic. The location of each of the symbols shown on figure 5 is thus determined not only with respect to the sonic point x_w^*, but also with respect to the airfoil. They range from a station 0.07 chord lengths upstream to a station 1.15 chord lengths downstream of the leading edge for the case in which H is 4.9 and from 0.05 to 0.93 chord lengths downstream of the leading edge for the case in which H is 3.1. The downstream station in both cases is, of course, the sonic point. A result of particular interest is the rapidity with which the values of $C_p/C_{p_{ch}}$ and $(1-M)/(1-M_{ch})$ increase from zero at the sonic point toward unity associated with conditions infinitely far upstream. It may be observed, in particular, that this process is about four-fifths completed at a point on the wall opposite the leading edge of the airfoil in each of the special, but not untypical, cases considered by Morioka.

COMPARISON OF EXPERIMENTAL AND THEORETICAL RESULTS

Consideration of the theoretical results summarized in the preceding section leads naturally to questions concerning the accuracy of the quantitative results, the general applicability of the qualitative results, and most of all, the degree to

which results of tests conducted in a conventional solid-wall wind tunnel operating in the choked condition can be used in the investigation of essentially unbounded flows with free-stream Mach number 1. Insight into the answers to these questions is sought in the following discussion by examination of a number of comparisons of experimental and theoretical results for representative airfoils.

Double-wedge airfoil.—Consider first the case of a nonlifting symmetrical double-wedge airfoil in a choked wind tunnel, for which the pertinent quantitative theoretical results are summarized in the preceding section. Figure 6 presents the results for the pressure distribution on the airfoil surface for a particular example of such a case in which a 10-percent-thick airfoil with a 4-inch chord is mounted on the center line of a test section of rectangular cross section having a height of only 4½ inches. This example represents an extreme case of a relatively large model in a small wind tunnel, and is useful to consider here because the wall-interference effects are displayed in a clear and pronounced manner.

Several sets of results are included on figure 6. The solid line represents the theoretical pressure distribution on the surface of a 10-percent-thick double-wedge airfoil in an unbounded flow with free-stream Mach number 1, and the broken line represents the corresponding result for the same airfoil in a choked wind tunnel having the relative dimensions stated in the preceding paragraph. These pressure distributions are calculated using the theoretical results of Guderley and Yoshihara and of Marschner that are summarized in more general form in equations (12) and (13) and in figures 3 and 4. These results also lead to a theoretical value for the choking Mach number M_{ch} of 0.695 for the conditions of this particular example.

The data points shown in figure 6 represent experimental values for C_p^* determined from tests conducted under choking conditions and reported by Nelson and Bloetscher in reference 21. Three sets of points are presented indicating the results measured with different pressure ratios across the test section. In each case, however, the static-pressure measurement on the wall upstream of the model indicates the same value for the choking Mach number, namely, 0.70.

The pressure distributions indicate, and the schlieren photographs given by Nelson and Bloetscher confirm, that a normal shock wave is situated about midway along the chord of the rear wedge when the pressure ratio across the test section is just sufficient for choking to occur. Increasing the pressure ratio results in a rearward movement of the shock wave across the chord, but almost no change in the pressure distribution upstream of the shock wave, much as in the very closely related case of flow in a Laval nozzle. At the highest pressure ratio, the normal shock wave has moved downstream of the airfoil and only an oblique shock remains extending downstream from the trailing edge. The latter case is more representative of the situation that arises in the course of typical wind-tunnel testing in which the dimensions of the test section are much larger with respect to those of the model than in the present example. These observations serve to call attention to the fact that it is necessary, when using a choked wind tunnel to simulate unbounded flows with free-stream Mach number 1, to assure that the pressure ratio across the test section is sufficient not only to assure choking, but also to force the shock wave to move either to its most rearward station or to a station downstream of the region of interest.

It is evident from the theoretical results summarized in the preceding sections that the dimensions of the model in this particular investigation are too large with respect to those of the test section for C_p^* measured under choking conditions to resemble closely the values for C_p in an unbounded flow with free-stream Mach number 1. It may be observed, however, that the theoretical and experimental results for both C_p^* and M_{ch} in the choked wind tunnel are in essential agreement. Even this agreement is somewhat surprising in view of the fact that the size of the model relative to the test section and the magnitude of the velocity perturbations, particularly upstream of the model, appear to be too large to be compatible with the small disturbance approximations fundamental to the theory. It should be noted, however, that many similar cases have been observed previously in the course of comparison of theoretical and experimental results for flows that are essentially unbounded (see ref. 3 for a résumé).

It is of interest, before leaving the present topic, to compare the results shown in figure 6 with the

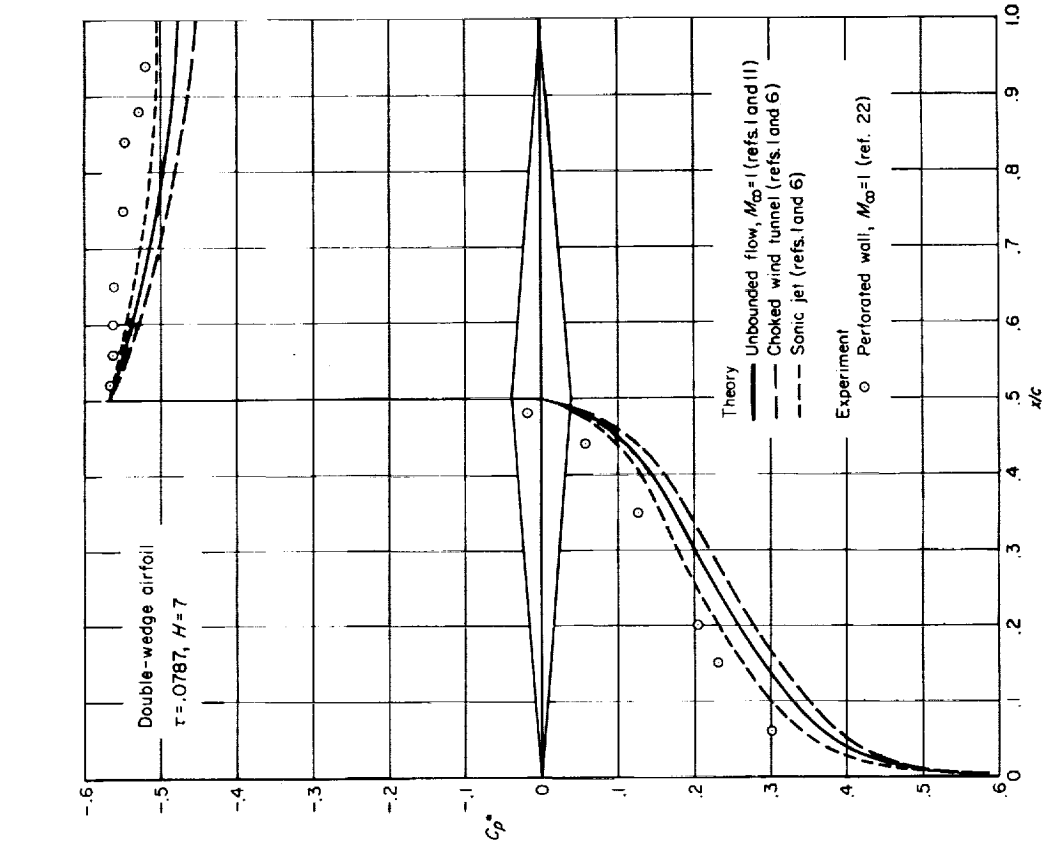

FIGURE 7.—Experimental and theoretical pressure distributions for a symmetrical double-wedge airfoil.

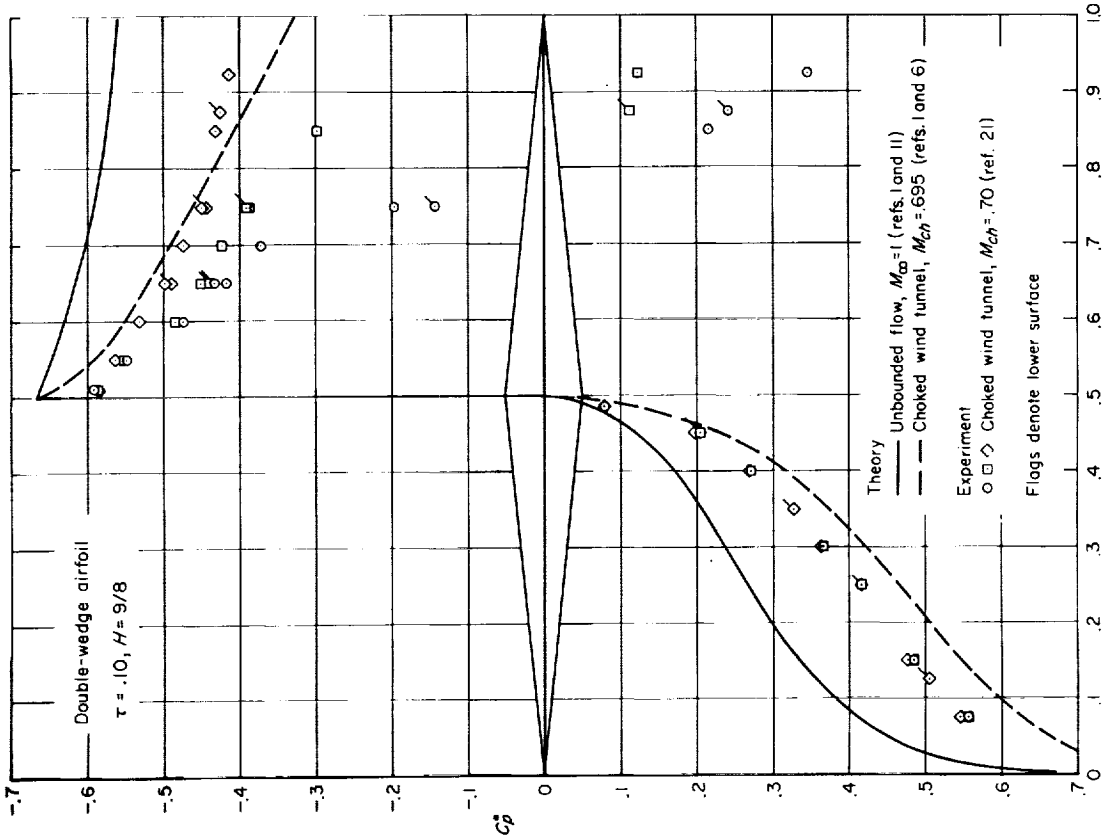

FIGURE 6.—Experimental and theoretical pressure distributions for a symmetrical double-wedge airfoil in a relatively small choked wind tunnel.

corresponding experimental results given by Knechtel in reference 22 for the pressure distribution at Mach number 1 on a 7.87-percent-thick double-wedge airfoil of 5-inch chord in a two-dimensional transonic wind tunnel having perforated walls with 5-percent open area. The dimensions of the cross section of this wind tunnel are 35 by 12 inches. The experimental results for this particular case are shown in figure 7 together with the corresponding theoretical results of Guderley and Yoshihara (ref. 11) for the same airfoil in an unbounded flow with free-stream Mach number 1, and of Marschner (ref. 6) for the same airfoil in both a choked solid-wall wind tunnel and in a sonic free jet. The latter results are given by an expression identical to equation (12) except for the replacement of the coefficient 1.802 by -2.037. It is to be anticipated that the theoretical pressure distribution for the airfoil in a transonic wind tunnel with partly open walls would fall somewhere between those for the open jet and the solid wall. Examination of the results shown on figure 7 reveals, however, that the experimental results differ from the theoretical results for an unbounded flow by an amount that exceeds the theoretical amount for an open jet. Although the discrepancies are reasonably small, when viewed in terms of uncertainties that usually prevail in transonic wind-tunnel testing, they may be significant since they appear to be at least qualitatively similar to those observed in a large number of similar comparisons in reference 9. It does not appear that all of the differences can be attributed to the wind-tunnel wall interference, however, inasmuch as the results of tests in a choked solid-wall wind tunnel shown in figure 6, as well as additional comparisons with the experimental data of Liepmann and Bryson given in reference 23, all display discrepancies of the same general nature. A possible additional source for part of the discrepancies may be associated with conditions in the vicinity of the sharp shoulder of the double-wedge airfoil, where the calculated results display an infinite pressure gradient in violation of the assumption of small perturbations fundamental to the theory, and where viscous effects of substantial magnitude may be expected to occur.

Circular-arc airfoil.—Further insight into the degree to which the pressure distribution on an airfoil in a choked solid-wall wind tunnel corresponds to that for an unbounded flow with free-stream Mach number 1 can be gained by examination of the results presented in figure 8 for a nonlifting circular-arc airfoil. The experimental results are from measurements reported by Knechtel in reference 22 of the pressures on a 6-percent-thick airfoil of 6-inch chord in the 35- by 12-inch two-dimensional transonic wind tunnel referred to in the preceding paragraph. Two sets of data points are shown on this plot with the axes displaced from each other for clarity of presentation. The lower set of points represent the experimental results obtained with the wind tunnel operating in the normal manner with the perforations open and an indicated Mach number of 1 in the test section. The upper set of points represents the experimental data obtained with the same model in the same wind tunnel, but with the perforations sealed and the tunnel operating in the choked condition. The curves represent the theoretical pressure distribution indicated by an approximate solution of the equations of transonic flow theory given in reference 23 for unbounded flow with free-stream Mach number 1 past a 6-percent-thick circular-arc airfoil. The two curves represent the identical results for the two coordinate systems, and serve as convenient reference lines in the comparison of the two sets of experimental data.

It can be seen that the various results included in figure 8 are in substantial agreement, although certain systematic differences are clearly visible. The differences are small, however, and it is difficult, in view of the approximate nature of the theoretical results and the undoubted presence of interference effects in the experimental results to form any definite conclusions regarding the relative merits of the three sets of results. It may, nevertheless, be of significance to note that a major part of the differences is consistent with properties of both the experimental and theoretical results that have been observed previously in other connections. It may be noted, for instance, that the experimental results from the tests with the perforations open indicate values for C_p that are slightly more negative at nearly all points along the chord than those from the tests with the perforations closed and the tunnel operating in the choked condition. The difference is qualitatively consistent with the theoretical results of Marschner for the double-wedge airfoil, with the theoretical expression given in reference 4 for wall-

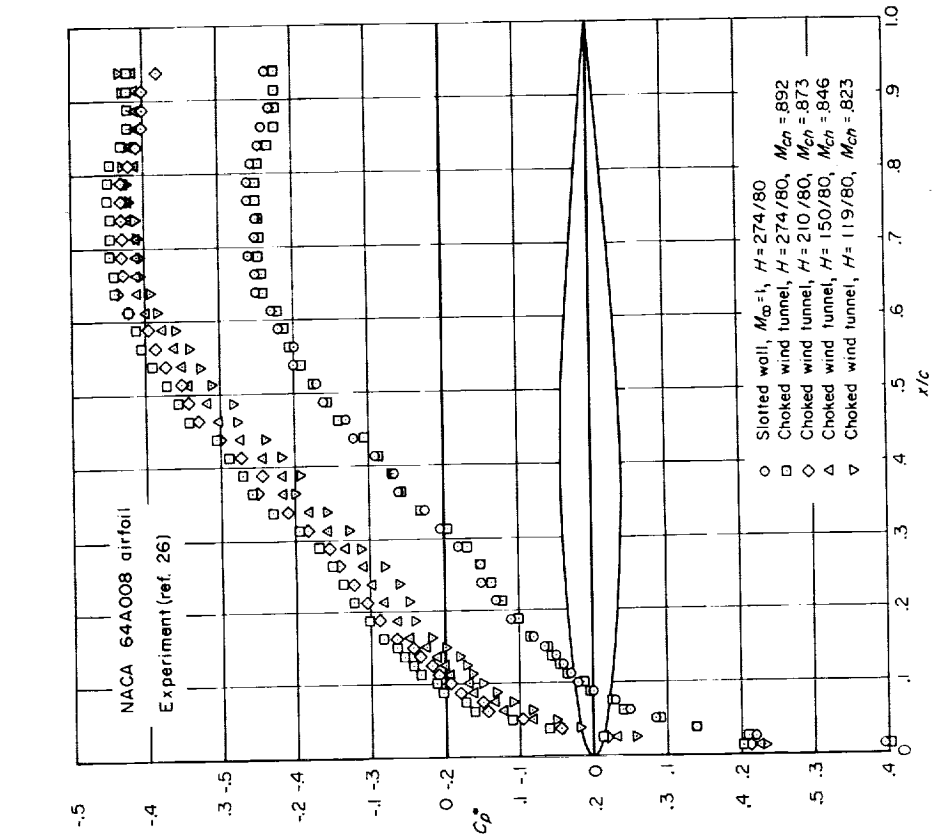

FIGURE 9.—Experimental pressure distributions for an NACA 64A008 airfoil in four choked wind tunnels of different dimensions and in a transonic wind tunnel.

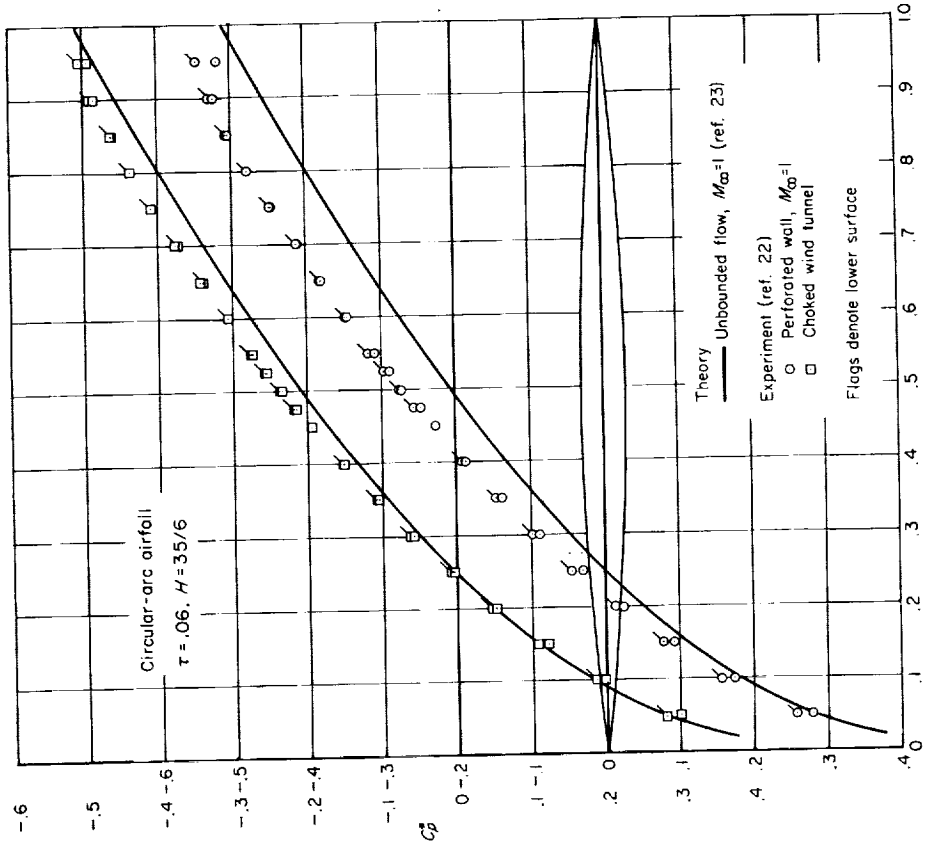

FIGURE 8.—Experimental and theoretical pressure distributions for a nonlifting circular-arc airfoil.

interference effects for transonic wind tunnels with porous or perforated walls, and with the general observation that most transonic wind tunnels seem to exhibit wall-interference effects at Mach number 1 that more or less resemble those of sonic jets. These considerations suggest that the values for C_p for an unbounded flow with free-stream Mach number 1 are somewhere intermediate between the two sets of experimental results shown in figure 8, and are thus slightly greater in magnitude over the rear part of the airfoil than the values indicated by the approximate theory of reference 23. Such a conclusion is consistent with the observed properties of an approximate solution calculated by the method of reference 23 for an airfoil only slightly different from a 6-percent-thick circular-arc airfoil that is presented in reference 3 together with the corresponding results for the same airfoil calculated by Nocilla (ref. 24) using the more accurate mathematical model for transonic flow proposed by Tomotika and Tamada in reference 25. Consideration of these and similar observations leads to the tentative conclusion that the results from the choked wind tunnel are perhaps as close to the desired results for an unbounded flow with free-stream Mach number 1 as any of the three sets of results shown in figure 8.

NACA 64A008 airfoil.—A set of experimental results illustrating the effect of the relative size of the model and the test section on the pressure distribution measured in a choked wind tunnel is presented in figure 9. These results, which are obtained from reference 26 by Larson and Sörensén, are for two-dimensional flow past a nonlifting NACA 64A008 airfoil of 80-millimeter chord, and the tests were conducted in five alternate test sections inserted as liners within the larger test section of a single wind tunnel. One of the liners has slotted walls with 2-percent open area, so that the test section simulates that of a transonic wind tunnel having dimensions 274 by 78 millimeters. The data from the measurements made in this test section at an indicated Mach number of 1 are represented by circles in the lower part of figure 9. The other liners had solid walls, and the remainder of the data shown in figure 9 was obtained with the tunnel operating in the choked condition. The dimensions of the largest of the four test sections with solid walls, for which the results are indicated by squares in both the upper and lower parts of figure 9, are the same as those of the slotted test section. The other test sections are all of the same width, 78 millimeters, but the inserts were installed so that the height was reduced to 210, 150, and 119 millimeters. Larson and Sörensén were concerned primarily with a study of the effects of the wall boundary layers, and presented many results in reference 26 for cases in which the thickness of the boundary layers on the liners with solid walls were artifically increased. Although the effects on the pressures on the airfoil surface were generally found to be very small, only those measurements obtained with the thinnest boundary layers for each wall configuration are used in the present paper. No theoretical pressure distribution for an NACA 64A008 airfoil in either bounded or unbounded flow with free-stream Mach number 1 is available at the present time for inclusion with the experimental results of figure 9.

It can be seen from an examination of the data shown in figure 9 that the results from the tests in the largest test section with solid walls are almost identical with those from the tests in the slotted test section, and that the results in the smaller test sections deviate a small, but significant amount from those in the larger test sections. It is interesting to observe that the differences between the results measured in the various test sections with solid walls are in almost perfect agreement with the predictions of the similarity rule given by equation (8), which states that the difference between the results measured in the 150 and the 210 millimeter test sections should be very nearly equal to the difference between the results measured in the 119 and 150 millimeter test sections, and that the difference between the results measured in the 210 and 274 millimeter test sections should be about three-fifths of the same quantity.

These same considerations indicate that the results from the 274 millimeter test section are not entirely free of significant wind-tunnel wall interference, and that the interference-free pressure distribution should be indicated in figure 9 by a curve displaced in the upward direction from the data points for the 274 millimeter test section by an amount that is very nearly equal to the difference between the results for the 274 and 150 millimeter test sections. The application of such a correction would, of course, destroy to a slight degree the nearly perfect agreement that

exists in figure 9 between the pressure distributions measured in the largest test section with solid walls and in the test section with slotted walls. It is important to realize, however, that the results in the slotted test section should not be taken as a definite standard for unbounded flow with free-stream Mach number 1, since they too are influenced by wind-tunnel wall interference that depends not only on the relative dimensions of the model and the test section, but also on the details of the design and construction of the partly open walls. This matter may be of particular significance in the present case, since the ratio of open to closed area is only 0.02 for the test section in which the data of figure 9 were measured, whereas that of most transonic wind tunnels is considerably greater.

Larson and Sörensén also include data in reference 26 for the pressure distribution on the same NACA 64A008 airfoil measured in slotted test sections of various heights having ratios of open to closed area of 0.02, 0.04, and 0.08. The results for the largest test sections, all of which have a height of 274 millimeters, are shown in figure 10. It can be seen that the pressure distributions change in a systematic manner with the ratio of open to closed area and that the values for C_p^* become more negative over most of the airfoil as this ratio is increased. Such a behavior is consistent with the known theoretical and experimental results for a sonic jet, which corresponds to the limiting case of a transonic wind tunnel with completely open walls.

The example given in the preceding paragraph illustrates the uncertainty that prevails in precision testing in transonic wind tunnels with partly open walls. It is of interest, before leaving this topic, to present additional experimental results from reference 26 to show some of the difficulties that arise in even the detection of the presence of significant wall interference in such wind tunnels. The results are presented in three sets with displaced axes in figure 11. Each set of results represents data obtained with a single model and with a single ratio of open to closed area, but with test sections of different height. It can be seen that the pressure distributions measured on the forward part of the airfoil in test sections of different size but of a single ratio of open to closed area tend to be in agreement, but that the results obtained in test sections of different ratio of open to closed area differ significantly from each other. This observation, together with the fact that the pressures on the forward part of an airfoil at free-stream Mach number 1 are independent of the shape of the rear part of the airfoil over a wide range of variations, clearly illustrates the important effects associated with the details of the construction of the walls of the test section of a transonic wind tunnel. It is also apparent that these effects may be of sufficient significance to introduce difficulties in the experimental assessment of the magnitude of wall-interference effects in transonic wind tunnels by the usual method of testing different size models in a single test section. It can also be seen that the pressure distributions measured on the rear part of the airfoil vary appreciably as both the dimensions of the test section and the ratio of open to closed area are changed, and that the pressures become more positive, in general, as the size of the test section is reduced and as the ratio of open to closed area is increased. The effects observed with the smaller and more open test sections are probably associated with wave reflection phenomena in which expansion waves emanating from the forward part of the airfoil are not perfectly canceled by the slotted wall, but are reflected back to the model as compression waves, more or less as from the boundaries of an open jet. The relative magnitudes of the incident and reflected waves depend, of course, on the details of the geometry of the walls. The nature of the resulting interference effects on the pressure distribution is quite different from that experienced on the forward part of the airfoil, however, and the apparent attainment of small interference effects on one part of the airfoil is no guarantee that interference effects are small on other parts.

The choking Mach number is also a quantity of interest, and Larson and Sörensén give the measured values for each of the cases for which the pressure distribution is shown in figure 9. They are 0.892, 0.873, 0.846, and 0.823, with the value for the largest test section listed first. These results are shown in figure 12 in terms of a plot of $1-M_{ch}$ versus the two-fifths power of the chord-height ratio, as suggested by the transonic similarity rule given by equation (9). The results should form a straight line through the origin. It can be seen that the four experimental points do, in fact, determine a reasonably straight

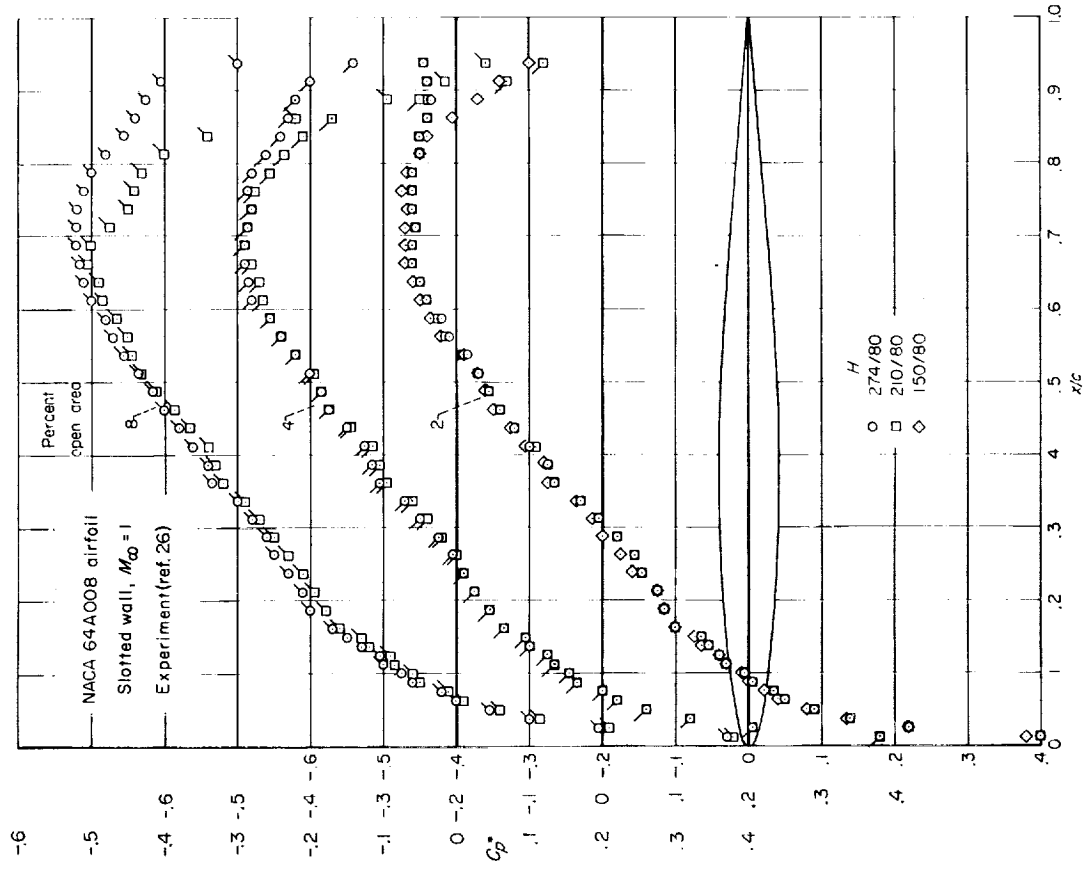

FIGURE 11.—Effect of the ratio of model to test section size on the pressure distributions measured on an NACA 64A008 airfoil in transonic wind tunnels with slotted walls.

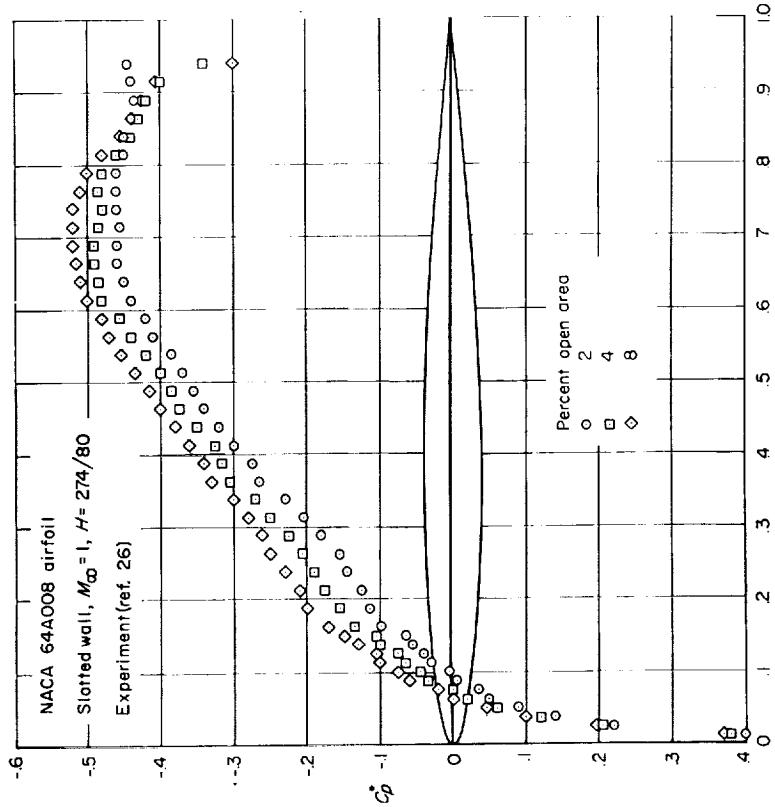

FIGURE 10.—Effect of the ratio of open to closed area on the pressure distributions measured on an NACA 64A008 airfoil in a transonic wind tunnel with slotted walls.

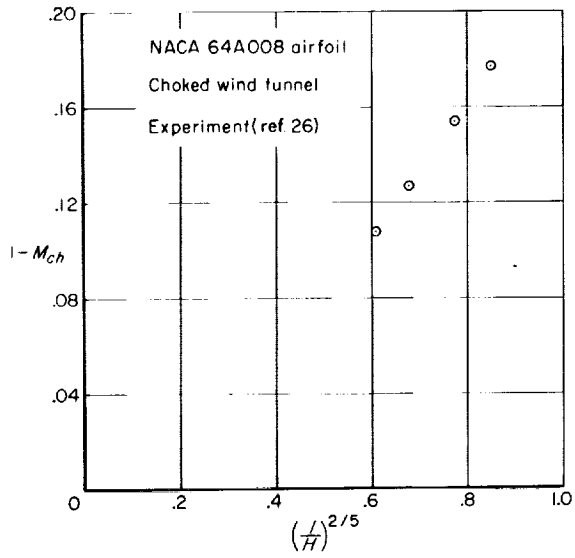

FIGURE 12.—Variation of choking Mach number with the two-fifths power of the chord-height ratio for an NACA 64A008 airfoil.

line, but that its extension does not pass through the origin. The reason for this discrepancy is not known, but it is probably significant that additional results given in reference 26 indicate that the choking Mach number is influenced to a substantial degree by the thickness of the boundary layer, and that the choking Mach number decreases in each of the test sections as the boundary-layer thickness is increased.

ADDITIONAL REMARKS FOR TWO-DIMENSIONAL FLOW

It is possible to utilize results available in scattered publications to provide several additional examples in which two-dimensional experimental results from solid-wall wind tunnels operating in the choked condition are compared with those from transonic wind tunnels with partly open walls. Interference effects of the wave reflection type are seldom of significance in two-dimensional tests involving models and test sections of the usual proportions, and it is found that the agreement between the results is generally about the same as that illustrated in the preceding examples provided, of course, that sufficient power is applied in the choked wind tunnel to force the shock wave to either its most downstream position or to a position downstream of the region of interest. A set of results that illustrates the magnitude of the effects that may be encountered when insufficient power is applied in tests more typical of customary wind-tunnel practice than those described in connection with figure 6 is presented in figure 13. These results are from reference 26 by Larson and Sörensén and represent once again the values for C_p^* measured on the surface of an NACA 64A008 airfoil of 80 millimeter chord in a test section having a height of 274 millimeters. All of the measurements are from tests conducted with the test section operating in a nominally choked condition, but the indicated choking Mach number varies through a range extending from 0.870 to 0.892. It is evident from these results, and also from the corresponding results for the double-wedge airfoil given in figure 6, that the use of a choked solid-wall wind tunnel to simulate unbounded flow with free-stream Mach number 1 may require the application of power somewhat in excess of that sufficient for the bare attainment of choked flow in the test section.

Results from a choked wind tunnel can sometimes be used to determine the pressure distribution on the entire airfoil even when sufficient power is not available by discarding the measured pressure distribution over the rear part of the chord and replacing it by a calculated pressure distribution determined by application of simple wave theory. Such a calculation can be based on the exact relations from the Prandtl-Meyer solution for flow around a corner, but it is frequently more convenient and almost as accurate to use the following approximate relation derived in reference 23 from the corresponding solution of the equations of the small disturbance theory of transonic flow:

$$C_p^* = -\frac{2\tau^{2/3}}{(\gamma+1)^{1/3}}\left\{\left[-\frac{(\gamma+1)^{1/3}C_p^*(X)}{2\tau^{2/3}}\right]^{3/2} - \frac{3}{2\tau}\left[Y'(x)-Y'(X)\right]\right\}^{2/3} \quad (14)$$

where Y' refers to dY/dx, X refers to the coordinate x of the station at which the calculated and measured results are joined, and $C_p^*(X)$ and $Y'(X)$ refer to the values for C_p^* and Y' at X. As noted in reference 23, the pressures computed over the rear part of the airfoil with either the exact or approximate expressions for simple wave theory tend to be somewhat too negative because the influence of the family of incoming compression waves arising from the sonic line is disregarded.

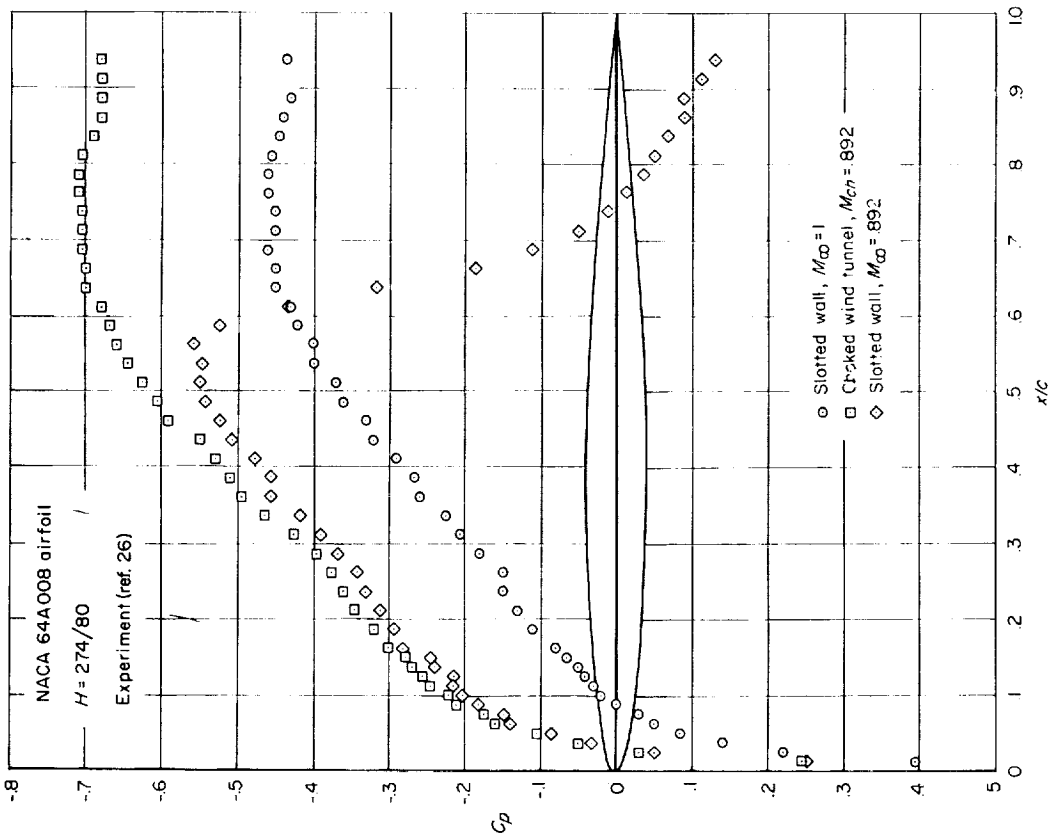

FIGURE 14.—Comparison of pressure distributions measured in a choked wind tunnel and in a transonic wind tunnel and expressed in terms of the pressure coefficient C_p for an NACA 64A008 airfoil.

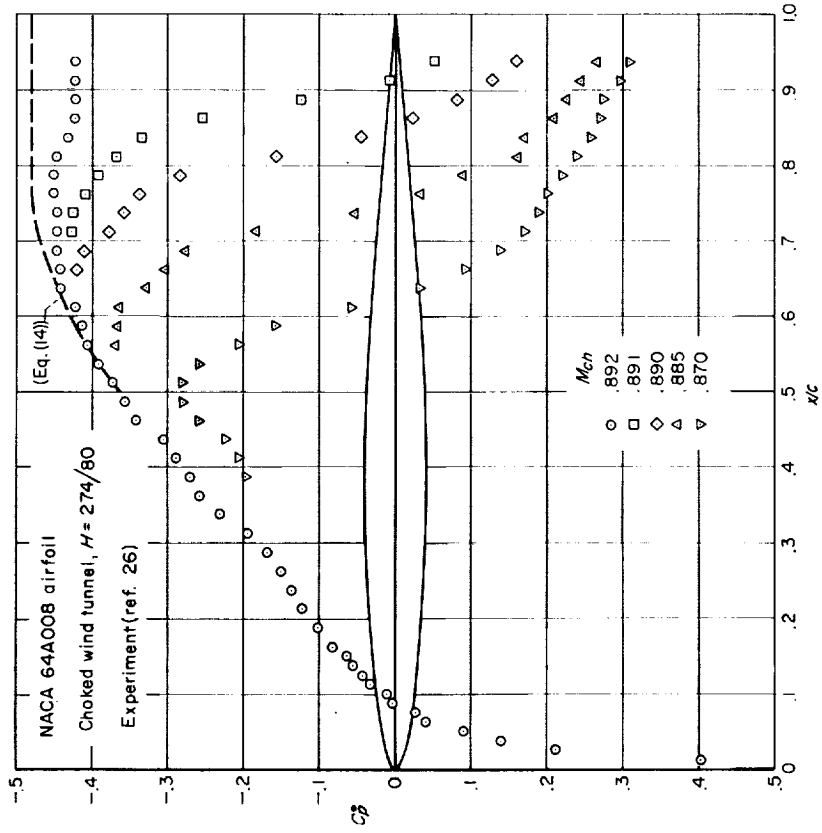

FIGURE 13.—Experimental pressure distributions for an NACA 64A008 airfoil in a solid-wall wind tunnel at several Mach numbers near choking.

The error is small in most cases, however, since the calculated results are applied to only a relatively small region near the trailing edge. An example of the results obtained by application of this procedure for the computation of the pressure distribution on the rear part of an airfoil is provided by the dashed line in figure 13. These results have been computed using equation (14) together with the experimental value shown in figure 13 for $C_p^*(X)$ at the midpoint of the airfoil at the largest choking Mach number. It can be seen that the results computed by this simple procedure are in relatively good agreement with the experimental pressure distribution observed at the largest choking Mach number, which has, in turn, been shown to be a good approximation for the pressure distribution on an NACA 64A008 airfoil in an unbounded flow with free-stream Mach number 1.

It should be emphasized before closing this discussion that the attainment of agreement between pressure distributions on an airfoil and a choked wind tunnel and in an unbounded flow with free-stream Mach number 1 requires that the wind-tunnel data be presented in terms of C_p^*, or some other quantity such as the local Mach number or the ratio of static pressure to stagnation pressure, that does not involve the use of the static pressure measured upstream of the model as a reference pressure. This requirement excludes, in particular, the use of the ordinary pressure coefficient C_p that is conventionally employed for the presentation of most wind-tunnel data. Figure 14 has been included to illustrate the nature of the comparisons that are observed between the results shown in the lower part of figure 9 for the solid and slotted test sections 274 millimeters in height when the pressure distributions are represented in terms of C_p. It can be seen that the two sets of results are displaced from each other by an amount that is nearly constant across the chord, and that the agreement which is observed in figure 9 when the two sets of results are presented in terms of C_p^* no longer exists. A third set of results from reference 26 are included on figure 14 representing the values for C_p measured in the slotted test section at an indicated Mach number of 0.892. It can be seen that these results also differ substantially from those measured in the choked test section at the same indicated Mach number, as might be expected in view of the well-known conclusion that results obtained in a choked wind tunnel are not only quantitatively, but qualitatively, different from those in an unbounded flow with free-stream Mach number equal to the choking Mach number.

AXISYMMETRIC FLOW

The case of axisymmetric flow around a slender pointed body of revolution of arbitrary shape is considered next. Although this case, which represents the simplest example of flow past a three-dimensional body, is of considerable interest in its own right, it possesses an importance in the study of transonic flow that considerably exceeds that which is normally associated with axisymmetric flow. The reason is that the transonic equivalence rule (see ref. 3 for a résumé) relates the solution for three-dimensional flow around a slender body of arbitrary cross section to the solution for the simple problem of axisymmetric flow around an "equivalent" nonlifting body of revolution having the same longitudinal distribution of cross-section area.

SUMMARY OF PRINCIPAL THEORETICAL RESULTS

Consider axisymmetric flow of an inviscid compressible fluid past a slender body of revolution of length l and maximum diameter d placed as shown in figure 15 on the center line of a circular test section of diameter D having solid walls and operating

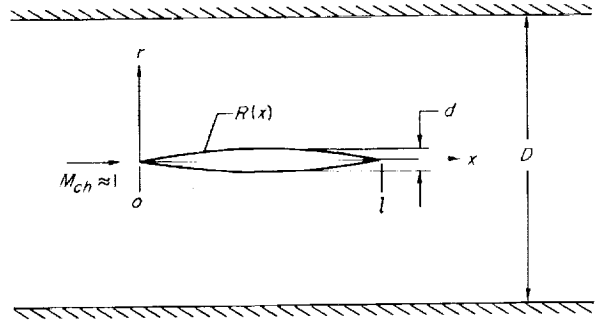

FIGURE 15. View of body of revolution, coordinate system, and principal dimensions.

in the choked condition. It is considered, just as in the preceding discussion of two-dimensional flow, that the diameter of the test section is sufficiently great that the choking Mach number is near unity, and the solution is developed in terms of deviations from conditions associated with a uniform flow with sonic velocity. Retention of only the leading terms in such a development leads

once again to the nonlinear equations of the small disturbance theory of nearly sonic axisymmetric flow. The principal equations of this theory are summarized below in terms of a cylindrical coordinate system oriented in such a way that the positive x axis extends in the downstream direction along the center line of the wind tunnel. The discussion of these equations and of some of the more pertinent results is organized in a manner that parallels that employed in the preceding section on two-dimensional flow, but is presented more briefly so as to eliminate unnecessary duplication and to focus attention more clearly upon the differences between axisymmetric and two-dimensional flows.

Basic equations.—Let U and V_r represent the components of the velocity parallel to the x and r axes, and define the perturbation velocity components u and v_r in such a way that $U=a^*+u$ and $V_r=v_r$. The quantities u and v_r can be expressed in terms of the gradient of a perturbation potential φ that satisfies the following nonlinear partial differential equation:

$$\varphi_{rr}+\frac{1}{r}\varphi_r=\frac{\gamma+1}{a^*}\varphi_x\varphi_{xx} \tag{15}$$

The boundary conditions for axisymmetric flow past a body in a choked wind tunnel are physically the same as those stated verbally in the preceding discussion of two-dimensional flow, but certain differences in nomenclature and in the behavior of the solution in the vicinity of the body make it necessary to rewrite the mathematical expressions for some of these conditions. The boundary conditions at the wind-tunnel wall and at the body that are given for two-dimensional flow by equations (2) and (3) are thus replaced by the following pair of expressions:

$$(\varphi_r)_{r=D/2}=0 \tag{16}$$

$$(r\varphi_r)_{r=0}=a^*R\frac{dR}{dx}=\frac{a^*}{2\pi}\frac{dS}{dx} \tag{17}$$

where $R(x)$ and $S(x)$ represent, respectively, the ordinates and cross-section area of the body. It is not necessary, on the other hand, to change the mathematical expression for the boundary condition represented by equation (4), and this relation applies equally to two- and three-dimensional flows. The expressions that relate the velocity and the two pressure coefficients C_p^* and C_p for axisymmetric flow are also somewhat different from the corresponding expressions for two-dimensional flow given by equation (5), and are as follows:

$$C_p^*=-\frac{2\varphi_x}{a^*}-\left(\frac{dR}{dx}\right)^2, C_p=-\frac{2\left[\varphi_x-(\varphi_x)_{x=-\infty}\right]}{a^*}-\left(\frac{dR}{dx}\right)^2 \tag{18}$$

Similarity rule.—The equations for axisymmetric transonic flow enumerated above contain a similarity rule that relates the flow fields associated with families of bodies of affinely related geometry in choked wind tunnels of arbitrary size. Various members of such a family of bodies may be of different length l and thickness ratio τ, but all must have ordinates given by an expression of the form $R/l=\tau f(x/l)$ where the thickness ratio must be small but is otherwise arbitrary, and the thickness distribution function $f(x/l)$ must be the same for all members of the family. If the subscripts 1 and 2 refer to two different members of a given family, the similarity rule states that the pressure coefficients at corresponding points defined by given values for x/l and $\tau r/l$ are related according to

$$\frac{C_{p_2}^*}{\tau_2^2}=\frac{C_{p_1}^*}{\tau_1^2} \tag{19}$$

provided the diameters of the two wind tunnels are related in accordance with the following expression:

$$\tau_2\overline{D}_2=\tau_1\overline{D}_1 \tag{10}$$

where $\overline{D}$ refers to the ratio D/l of the tunnel diameter to body length. The similarity rule also indicates the following relation between the choking Mach numbers for the two flows:

$$\frac{1-M_{ch_2}}{\tau_2^2}=\frac{1-M_{ch_1}}{\tau_1^2} \tag{21}$$

The similarity rule given above cannot be used directly to relate the surface pressures on bodies having different thickness ratios because the ordinates of related bodies do not conform with the relationship for corresponding points. Thus the r coordinate of a point in the vicinity of body 2 that corresponds to a point on the surface of body 1 is given by

$$\frac{r_2}{R_2}=\left(\frac{\tau_1}{\tau_2}\right)^2 \tag{22}$$

Oswatitsch and Berndt have shown in reference 27 that a similarity rule can be established for the surface pressures on affinely related bodies of revolution in unbounded flow if it is assumed that the longitudinal perturbation velocity component u is given by an expression of the form

$$u=\frac{a^*}{2\pi}\frac{d^2S}{dx^2}\ln r+g(x) \tag{23}$$

in the vicinity of the body. This relation permits the calculation of the difference in pressure between the point r_2 and the surface of body 2. Application of the same relation to the case of axisymmetric flow in a choked wind tunnel leads to the following similarity rule for the surface pressures:

$$C_{p_2}{}^*=\left(\frac{\tau_2}{\tau_1}\right)^2\left(C_{p_1}{}^*+\frac{2}{\pi}\frac{d^2S}{dx^2}\ln\frac{\tau_1}{\tau_2}\right) \tag{24}$$

provided still that the dimensions of the bodies and wind tunnels are related in accordance with equation (20). This rule can be expressed in functional form similar to that given by equation (6) for two-dimensional flow, in which case the appropriate expressions for the pressure coefficient and the choking Mach number are as follows:

$$\frac{C_p{}^*+(2/\pi)\,(d^2S/dx^2)\ln\tau}{\tau^2}=\mathrm{P}\left(\overline{D}\tau,\frac{x}{l}\right) \tag{25}$$

$$\frac{1-M_{ch}}{\tau^2}=\mathrm{M}\,(\overline{D}\tau) \tag{26}$$

Further insight into the interference effects in a choked wind tunnel within the region upstream of that influenced by wave reflection can be had in axisymmetric flow, just as in two-dimensional flow, if one considers the asymptotic behavior of the flow at great distances from the body. Guderley has examined this aspect of the present problem in references 1 and 28, and has shown that the deviation $\Delta C_p{}^*$ of the values for $C_p{}^*$ from the corresponding values $(C_p{}^*)_{\mathrm{M}_\infty=1}$ for the same body in an unbounded flow with free-stream Mach number 1 is proportional to $(1-\mathrm{M}_{ch})^{5/3}$ and inversely proportional to D/l' where l' is some length characteristic of the length of the part of the body that can influence the subsonic part of the flow. Combination of this result and the similarity rule leads to the following pair of relations for $\Delta C_p{}^*$ and M_{ch} for a family of affinely related bodies:

$$\frac{\Delta C_p{}^*}{\tau^2}=\frac{\mathrm{P}(x/l)}{(\overline{D}\tau)^{10/7}} \tag{27}$$

$$\frac{1-M_{ch}}{\tau^2}=\frac{Const}{(\overline{D}\tau)^{6/7}} \tag{28}$$

Equations (27) and (28) lead to a series of statements regarding the conditions under which a choked wind tunnel is useful for the simulation of an unbounded axisymmetric flow with free-stream Mach number 1. These statements are qualitatively similar to those given for two-dimensional flow following equations (8) and (9), but differ quantitatively with respect to the powers to which the various quantities appear in the results. One thus observes that the interference effects on the pressure distribution, as signified by the values for $\Delta C_p{}^*$, are inversely proportional to the 10/7 power of the ratio D/l of the diameter of the wind tunnel to the length of the body, and proportional to the 4/7 power of the thickness ratio, from which it follows that smaller errors result when smaller models are tested, and that the magnitude of the interference effects is smaller for thin bodies than for thick bodies. The quantity $(C_p{}^*)_{M_\infty=1}$ that is intended to be simulated is of the order of τ^2, however, and the result emerges that the relative error $(\Delta C_p{}^*)/(C_p{}^*)_{M_\infty=1}$ is inversely proportional to $\tau^{10/7}$, and is hence once again larger for thin bodies than for thick bodies. As in the case of two-dimensional flow, equations (27) and (28) indicate that the choking Mach number depends on a different combination $\overline{D}$ and τ than does $(\Delta C_p{}^*)/(C_p{}^*)_{M_\infty=1}$, from which it follows that the quality of the simulation of a three-dimensional, as well as two-dimensional, flow in a choked wind tunnel cannot be judged by the nearness to unity of the choking Mach number.

Although the distinction between l' and l has been dropped in writing the above relations, since the ratio of the two quantities is a constant for all members of an affinely related family of bodies, it should be noted just as in the case of two-dimensional flow that the total length and maximum thickness of the body are not the significant lengths associated with the wind-tunnel interference in a choked wind tunnel. It follows once again, from the fact that the dimensions of significance are those associated with the part of the body that can influence the subsonic part of the flow

field, that interference effects at Mach number 1 on a family of nonaffinely related smooth bodies of given length and thickness increase as the point of maximum thickness is moved rearward across the length.

Application to unbounded flow with free-stream Mach number 1.—The relations for axisymmetric flow in a choked wind tunnel given in the preceding sections reduce to the appropriate forms for unbounded flow with free-stream Mach number 1 as the diameter of the test section is increased to infinity. In such a case, the quantity $\overline{D}\tau$ grows beyond all bounds for a body of given geometry, and disappears as a significant parameter in the description of the flow. Although the resulting equations appear to be the simplest set of relations capable of describing axisymmetric transonic flows, the difficulties of solution are even greater than those associated with the equations for two-dimensional transonic flow, and no exact, or essentially exact, solutions exist for flow around a complete body at free-stream Mach number 1. One of the fundamental differences with the two-dimensional case is that the governing equations are not linearized by application of the hodograph transformation, and the difficulties associated with both the nonlinear character and the mixed type of the equations must be faced simultaneously. Inasmuch as the mathematical theory of such equations is still in a rather early state of development and methods have not yet been discovered for the exact solution of such equations, it is necessary to turn to approximate methods for the solution of practical problems. Several such approximate methods have been proposed in recent years for the solution of axisymmetric flow problems with free-stream Mach number 1. Of these, the most successful and also the most versatile method is that described briefly in references 3 and 29, and more completely in reference 30. The latter reference also includes brief reviews of many of the other approximate methods together with extensive comparisons of theoretical and experimental results for a variety of bodies. Most of the theoretical results to be presented in the remainder of this paper are either drawn directly from the latter reference or are new results calculated by application of the same procedures.

Application to flow in a choked wind tunnel.—Attention is called to the fact that all of the theoretical pressure distributions for bodies of revolution given in this paper are for unbounded axisymmetric flow with free-stream Mach number 1. No solutions, either exact or approximate, are presently available for the pressure distribution on a body of revolution in a choked wind tunnel. It is consequently not possible to employ purely theoretical considerations at the present time to determine quantitative information regarding the numerical magnitude of interference effects in axisymmetric flow in a choked wind tunnel. The magnitude of these effects is therefore investigated in the following discussion by comparison of theoretical results for an unbounded flow with free-stream Mach number 1 with experimental results measured both in choked wind tunnels and in conventional transonic wind tunnels having either slotted or perforated walls.

COMPARISON OF EXPERIMENTAL AND THEORETICAL RESULTS

It may be recalled that all of the experimental data presented in the preceding discussion of two-dimensional flows are obtained from the existing body of published literature. Although there is a great abundance of such data, and also a growing supply of data from transonic wind tunnels with partly open walls that provides information on the pressures on bodies of revolution at Mach number 1, there is very little published data that presents the corresponding results for axisymmetric flows that are measured under choking conditions in wind tunnels with solid walls. It has been necessary, therefore, to conduct a series of tests for the express purpose of acquiring such data. This has been done in the 12-Foot Pressure Wind Tunnel at Ames Research Center. The test section of this wind tunnel is essentially circular in cross section, with a diameter of 12 feet. The models were mounted in the test section on sting-type model supports that extend along the center line of the wind tunnel, and were tested at zero angle of attack with a tunnel stagnation pressure of about 5½ pounds per square inch absolute. Most of the models were not new, but were existing models available from previous tests in transonic wind tunnels at Ames Research Center. The models were repolished before testing, and a new set of orifices was installed in one of the models. Each of the models had two rows of static-pressure orifices located on opposite sides that extended from nose to base. Multiple-tube manometers

using water or tetrabromoethane (specific gravity =2.95) were photographed to record the pressure data. Static pressures were also measured simultaneously at several stations along the wall of the test section to insure that the region of supersonic flow extended to the wall and that the tunnel was choked.

Cone-cylinder. Consider first the case of a slender cone-cylinder. Figure 16 is a plot of the results of pressure-distribution measurements on two cone-cylinders. Both have a semiapex angle of 7°, but the diameter of one of the models is 1.35 inches and that of the other is 4.7 inches. Although the two sets of results are clearly distinguishable, the differences are relatively small.

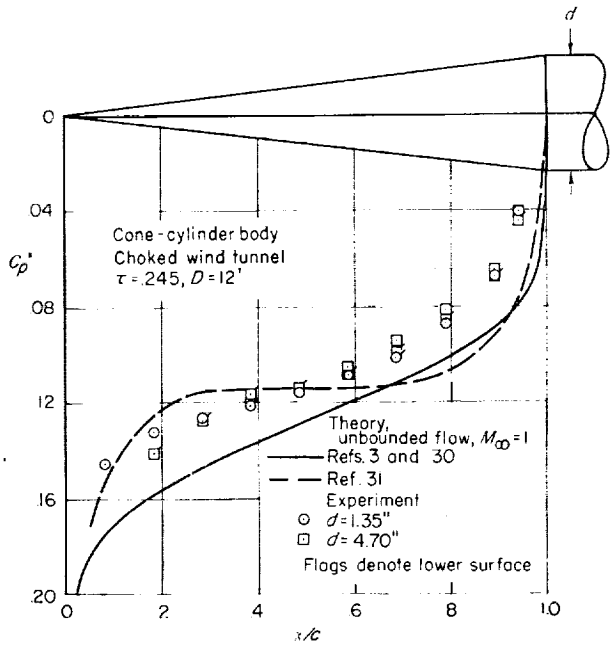

FIGURE 16.- Comparison of pressure distributions measured on two different cone-cylinders in a choked wind tunnel and two theoretical pressure distributions for unbounded flow with free-stream Mach number 1.

Consideration of this fact together with the results indicated by equation (27), that the interference effects on the smaller model should be only about 1/6 of those of the larger model, leads to the conclusion that the pressure distributions measured in these tests should be very nearly that associated with unbounded flow with free-stream Mach number 1. The solid line included in figure 16 indicates the theoretical pressure distribution given in references 3 and 30 for a 7° cone-cylinder in such a flow. It can be seen that the pressure distribution indicated by the theoretical curve is similar in form to that indicated by the experimental data, although displaced somewhat. The reason for this discrepancy is not known, but it may be significant to note that the nature of the discrepancy is similar in many respects to that observed in figure 7 for the front face of the double-wedge airfoil. It is again quite conceivable that conditions associated with the vicinity of the sharp shoulder may be responsible for a major part of the differences. Also included in this figure is a plot of the pressure distribution indicated by the numerical approximate solution of Yoshihara (ref. 31)[3] for a cone-cylinder with a semiapex angle of 1/10 radian transformed so as to be appropriate for a 7° cone by application of the similarity rule given by equation (24). It is evident that this result does not agree, even in form, with the other results shown in figure 16.

The results shown in figure 16 for the 7° cone-cylinder have an interest that exceeds that which would normally be associated with a particular body, since Page has shown in reference 2 that interference effects of surprisingly large magnitude are observed on the pressure distribution on such a body at Mach number 1 in tests in transonic wind tunnels with perforated walls. The smaller of the two cone-cylinders for which data are presented in figure 16 was tested by Page in two transonic wind tunnels of widely different size, namely, the Ames 2- by 2-Foot and 14-Foot Transonic Wind Tunnels. An interesting feature of these wind tunnels is that the smaller is the pilot model for the larger and that the dimensions of the test sections, which are square in cross section, and the construction of the perforated walls are very closely scaled with regard to both the proportion (5.4 percent) and distribution of the open and closed parts of the walls of the test section. The results of the tests are presented in figure 17 together with the two theoretical curves from figure 16. The experimental results measured in the two transonic wind tunnels are clearly different from each other and also from both of the theoretical results. In addition to the experimental results, Page presented the results of an approximate analysis of the interference effects

[3] A correction has been applied to Yoshihara's results to allow for a sign error in the quadratic term of the expression for C_p.

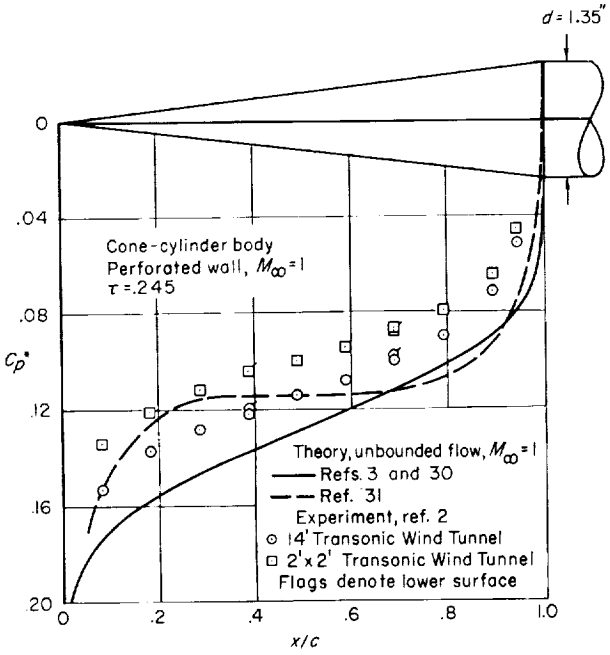

FIGURE 17.—Comparison of pressure distributions measured on a cone-cylinder in two different transonic wind tunnels and two theoretical pressure distributions for unbounded flow with free-stream Mach number 1.

at Mach number 1 in a transonic wind tunnel with porous or perforated walls. This analysis, which is patterned after a similar analysis for a transonic wind tunnel with slotted walls given by Berndt is reference 32, indicates that substantial interference effects occur in not only the results obtained in the smaller wind tunnels but also those obtained in the larger wind tunnel. It was shown further, in reference 2, that the corrected data from both tunnels are in very good agreement with each other over the rear half of the cone, but not over the front part. It was subsequently shown in reference 30 that application of Page's correction theory leads to a substantial improvement in the agreement with the theoretical pressure distribution developed in the same paper. The differences apparent among the various results over the front part of the cone are highlighted even more by these comparisons, however, and it was subsequently suggested in references 3 and 4 that the correction theory given by Page may not be entirely satisfactory. The various results shown in figures 16 and 17 tend to support this conjecture, and suggest furthermore that the interference effects on the results for the small cone in figure 16 and for the large wind tunnel in figure 17 are very small. Such a conclusion seems to be very reasonable in view of the unusually small size of the model relative to the test sections. It does leave a certain discrepancy between the best experimental and theoretical results unresolved, however, but it is quite possible that this may be associated with the conditions associated with the vicinity of the sharp shoulder as suggested in the preceding paragraph.

Parabolic-arc body.—The case of a parabolic-arc body of revolution represents an example of considerable interest because of the abundance of experimental and theoretical results. The results for the pressure distribution on the surface of several such bodies with thickness ratios that vary from 1/6 to 1/14 are presented in figures 18 through 21. These data represent not only the results of measurements in a choked wind tunnel with solid walls, but also the results of tests in a variety of transonic wind tunnels with both slotted and perforated walls. The results included in each of the figures are divided into two or three sets and for clarity of presentation are shown with displaced axes. Also included in each of these figures is the corresponding theoretical pressure distribution given in reference 30 for unbounded flow with free-stream Mach number 1. The curves representing the theoretical results are repeated for each of the axes on each of the figures so as to provide reference lines with which the various experimental results may be compared. It should be noted, however, that the theoretical results refer to pressure distributions on complete parabolic-arc bodies, whereas the experimental results refer to the pressure distributions measured on truncated parabolic-arc bodies mounted on cylindrical supports that extend downstream from the base of the model. The model supports, moreover, are not geometrically similar with respect to the bodies in the various tests, but are as indicated by the drawings along the axes used for the presentation of the corresponding experimental results. Although some effects of the model support would be expected to extend forward of the immediate vicinity of the base of the model, it is anticipated that these effects are small, and that the various results are comparable over nearly the full length of the experimental bodies.

The results for the parabolic-arc body of thickness ratio 1/6 are shown in three parts in figure 18.

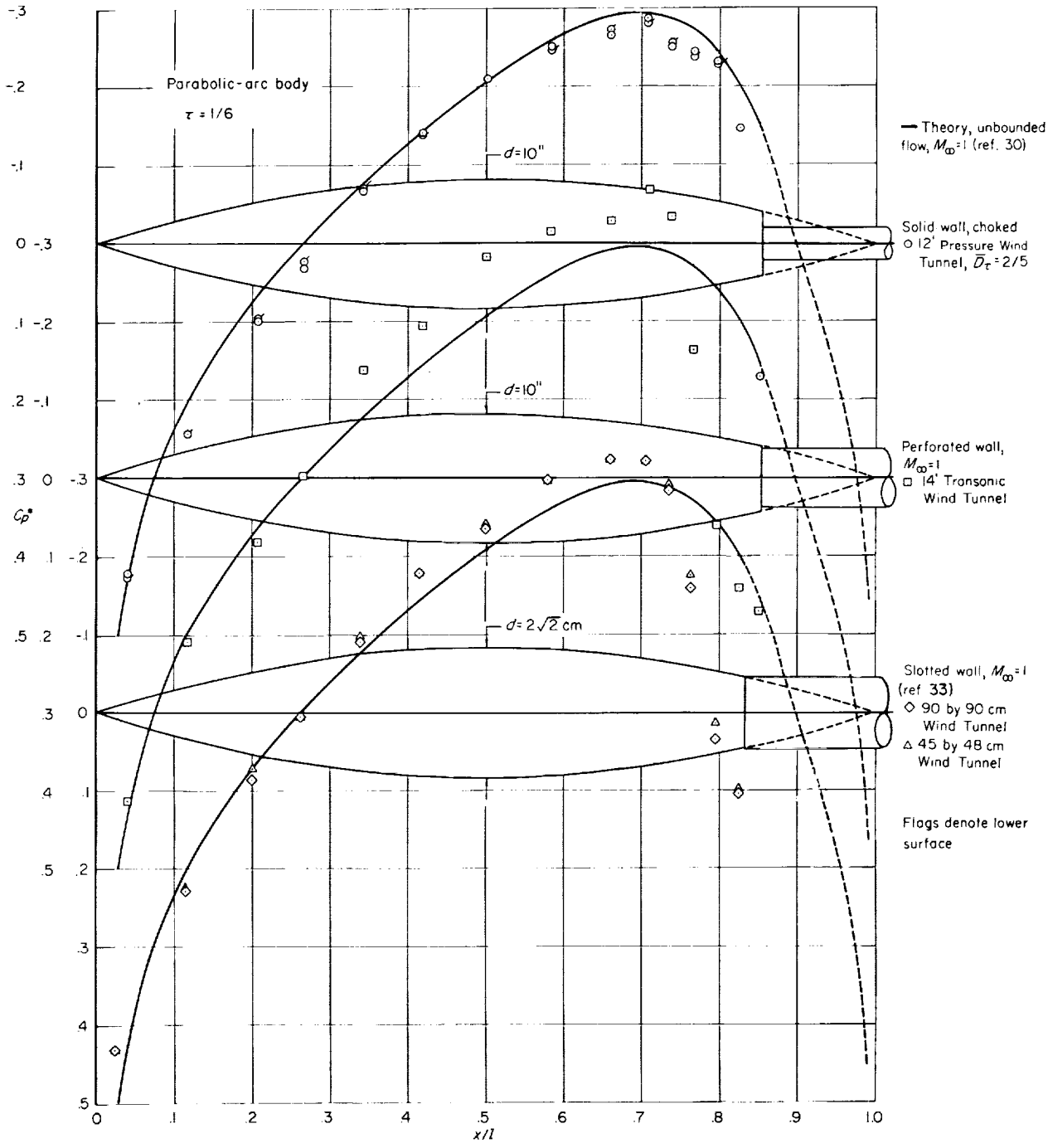

FIGURE 18.—Experimental and theoretical pressure distributions for parabolic-arc bodies of thickness ratio 1/6.

The experimental data presented in the upper part of this figure refer to the results obtained under choking conditions in the Ames 12-Foot Pressure Wind Tunnel for a body with a maximum diameter of 10 inches. The experimental data presented in the middle part of this figure refer to measurements made by Dannenberg at an indicated Mach number of 1 in the Ames 14-Foot Transonic Wind Tunnel with the same model as was used in the tests in the choked wind tunnel. The experimental data presented in the lower part of figure 18 are from reference 33 and refer to the results of measurements made by Drougge in transonic wind tunnels with two slotted walls using a body with a maximum diameter of $2\sqrt{2}$ centimeters. Two sets of data are included in this part of the figure. They represent the results obtained in two different wind tunnels, the test sections of which measure 90 by 90 centimeters and 45 by 48 centimeters.

It can be seen that the experimental results from the choked wind tunnel are in good agreement with the theoretical results for unbounded flow with free-stream Mach number 1. All of the results are in essential agreement with regard to the general nature of the pressure distribution on a parabolic-arc body of revolution at Mach number 1, but significant quantitative differences exist among the results of measurements in the various wind tunnels. As in the case of two-dimensional flow, the results from the transonic wind tunnels indicate values for the pressure coefficient that are slightly more negative than those from the choked wind tunnel. Of the various results from the transonic wind tunnels, those from the 90- by 90-centimeter wind tunnel would normally be expected to be most nearly interference-free since the dimensions of the model are substantially smaller relative to the dimensions of the test section than for any of the other models for which data are shown in figure 18. This fact, together with the observation that the data from the 90- by 90-centimeter wind tunnel are in better agreement with the theoretical results than are the data from the 14-Foot Transonic Wind Tunnel, leads to the conclusion that the theoretical pressure distribution indicated in figure 18, and hence also the experimental results measured in the choked wind tunnel, are very good approximations for the pressure distribution on a parabolic-arc body of revolution of thickness ratio 1/6 in an unbounded flow with free-stream Mach number 1.

The results shown in figure 18 have also been discussed from the point of view of an analysis of interference effects in transonic wind tunnels in references 3 and 4 where it is shown that application of Page's correction formula leads to a substantial improvement in the agreement among the results from the various transonic wind tunnels. It is also shown in these references, however, that the predictions indicated by the correction formula are not entirely satisfactory. The evaluation of proposed methods and the development of new methods for the prediction of interference effects in transonic wind tunnels is a subject somewhat apart from the principal goal of the present investigation, however, and attention in this paper will be confined, insofar as it is possible, to the simpler problem of the evaluation of the usefulness of the choked wind tunnel in the simulation of unbounded flow with free-stream Mach number 1.

The results shown in figure 19 for the pressure distribution on a parabolic-arc body of revolution of thickness ratio 1/12 furnish an interesting contrast with those given in the preceding figure. The theoretical results from reference 30 for an unbounded flow with free-stream Mach number 1 are presented in figure 19 together with two sets of experimental results, both for the same model which had a maximum diameter of 6 inches. The data presented in the upper part of this figure refer to the results obtained under choking conditions in the Ames 12-Foot Pressure Wind Tunnel. Those presented in the lower part refer to the results measured at an indicated Mach number 1 in the Ames 14-Foot Transonic Wind Tunnel and reported in reference 34 by Taylor and McDevitt. It can be seen that the relationships among the various experimental and theoretical results are substantially the same as for the body of thickness ratio 1/6 over the front part of the body, but that substantial discrepancies appear among the results at stations rearward of about 60 percent of the body length. The experimental data obtained in the choked wind tunnel are, moreover, generally on the opposite side of the theoretical curve from the experimental data obtained in the transonic wind tunnel with partly open walls.

Similar effects, although larger in magnitude, are immediately apparent in the corresponding

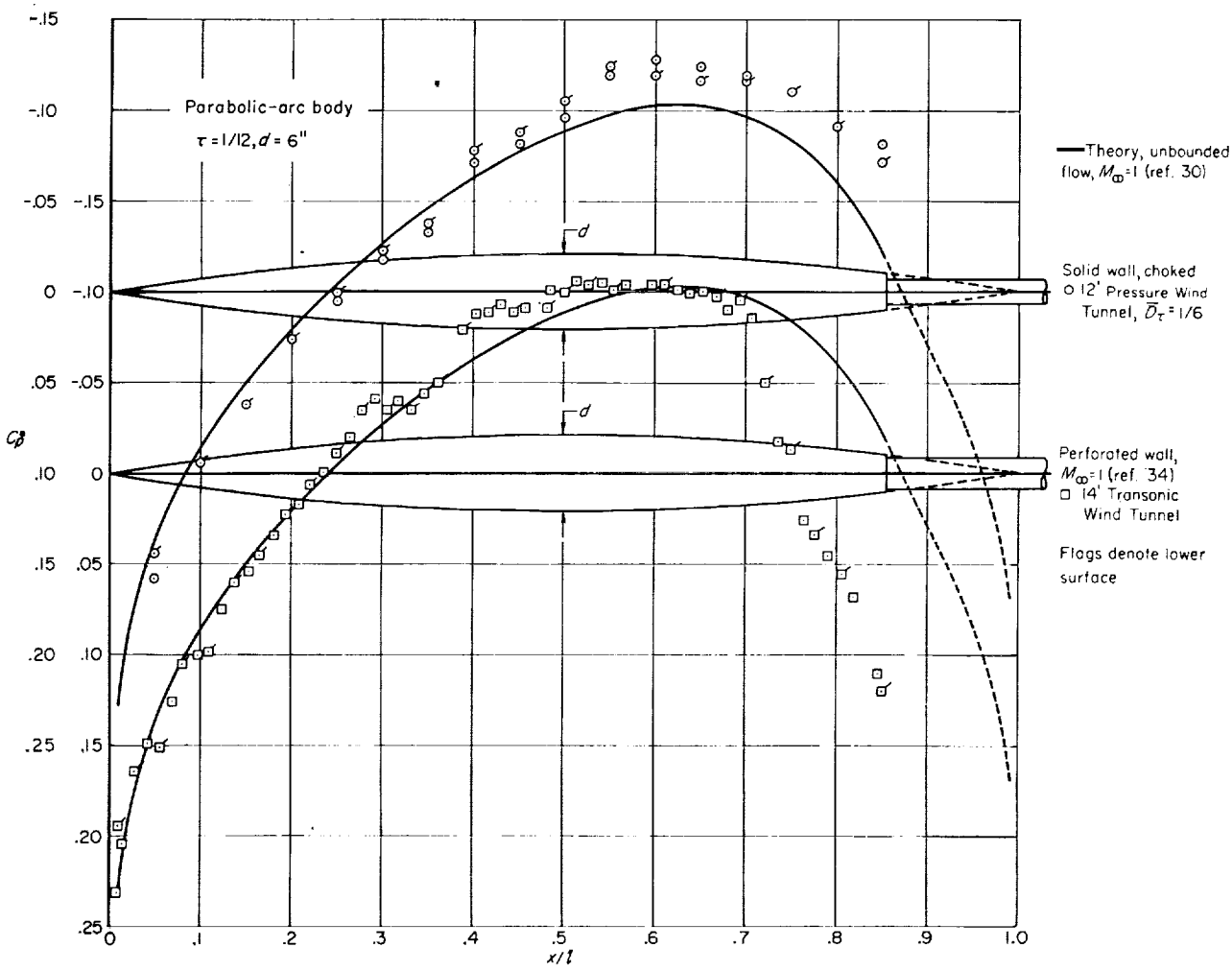

FIGURE 19.—Experimental and theoretical pressure distributions for parabolic-arc bodies of thickness ratio 1/12.

results presented in figures 20 and 21 for two different parabolic-arc bodies of thickness ratio 1/14 with maximum diameters of 6 and 8 inches. The magnitude of the interference effects observed in these results is so large, in fact, that the data from both the choked wind tunnel and the transonic wind tunnel are almost useless as an indication of the pressure distributions that occur on these particular bodies in an unbounded flow with free-stream Mach number 1.

Examination of the various results shown in figures 19 through 21 discloses a considerable variation for each body. The differences between a given pair of experimental and theoretical results are generally of opposite sign on the front and rear of each body, and are, moreover, of such a nature that the theoretical pressure distribution for unbounded flow with free-stream Mach number 1 is somewhere between the experimental results measured in the choked wind tunnel and those measured in the transonic wind tunnel. It can be seen, in particular, that the values for the pressure coefficient measured in the choked wind tunnel are too positive on the front of the body and too negative on the rear for agreement with the theoretical result. This observation, when considered together with the qualitative discussions presented in some of the preceding sections of this paper, provides a strong indication that interference effects of the type described in connection with equations (27) and (28) are present on the front of the bodies, but that these effects are overbalanced on the rear of the bodies by interference effects of the wave reflection type.

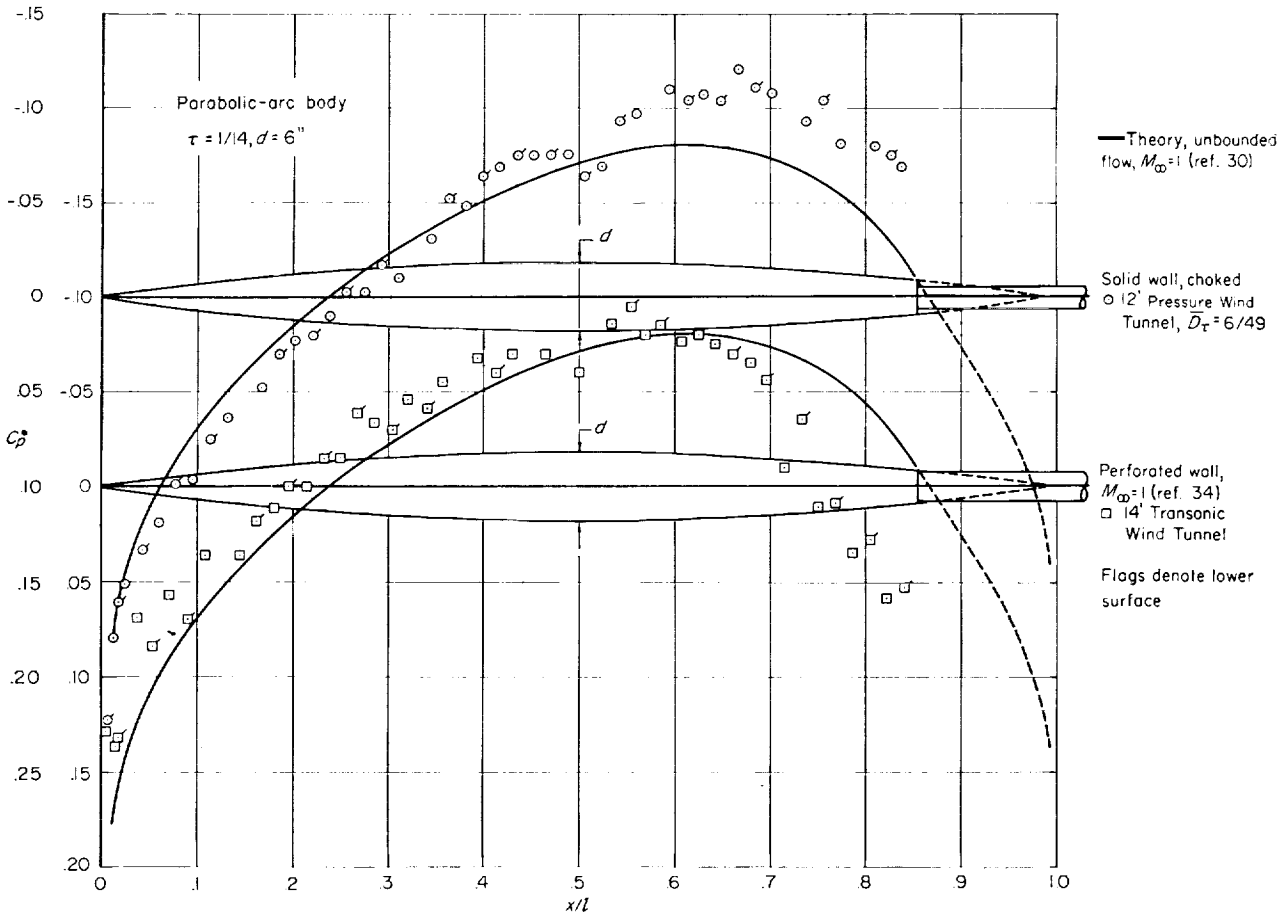

FIGURE 20.—Experimental and theoretical pressure distributions for parabolic-arc bodies of thickness ratio 1/14 and maximum diameter 6 inches.

A check on the validity of the first part of the preceding statement can be made by comparing the differences between the experimental results measured in the choked wind tunnel and the corresponding theoretical results for an unbounded flow with free-stream Mach number 1 with the predictions provided by the similarity rule given by equation (27). This rule, which states that the absolute magnitude of the interference effects on the pressure coefficient are proportional to $\tau^{4/7}/\overline{D}^{10/7}$, indicates that the interference effects are smallest for the body of thickness ratio 1/12, about 15 percent larger for the body of thickness ratio 1/6 and for the smaller body of thickness ratio 1/14, and about 70 percent greater for the larger body of thickness ratio 1/14. It can be seen that the differences among the various experimental and theoretical results are in at least qualitative agreement with these predictions over the front of each of the four bodies.

The validity of the statement that the interference effects on the rear of the bodies of thickness ratios 1/12 and 1/14 are due predominantly to wave reflection phenomena can be checked by examination of the characteristic diagram presented in figure 22. This diagram shows an abridged plot of the characteristic lines for an unbounded flow with free-stream Mach number 1 about a parabolic-arc body of thickness ratio 1/6. It is taken from reference 35 by Oswatitsch and has been calculated by use of the linearized theory of sonic flow described by Oswatitsch and Keune in reference 36 to compute the conditions along the sonic line, and by use of a simplified method of characteristics based on the nonlinear equations of transonic flow theory to compute the conditions

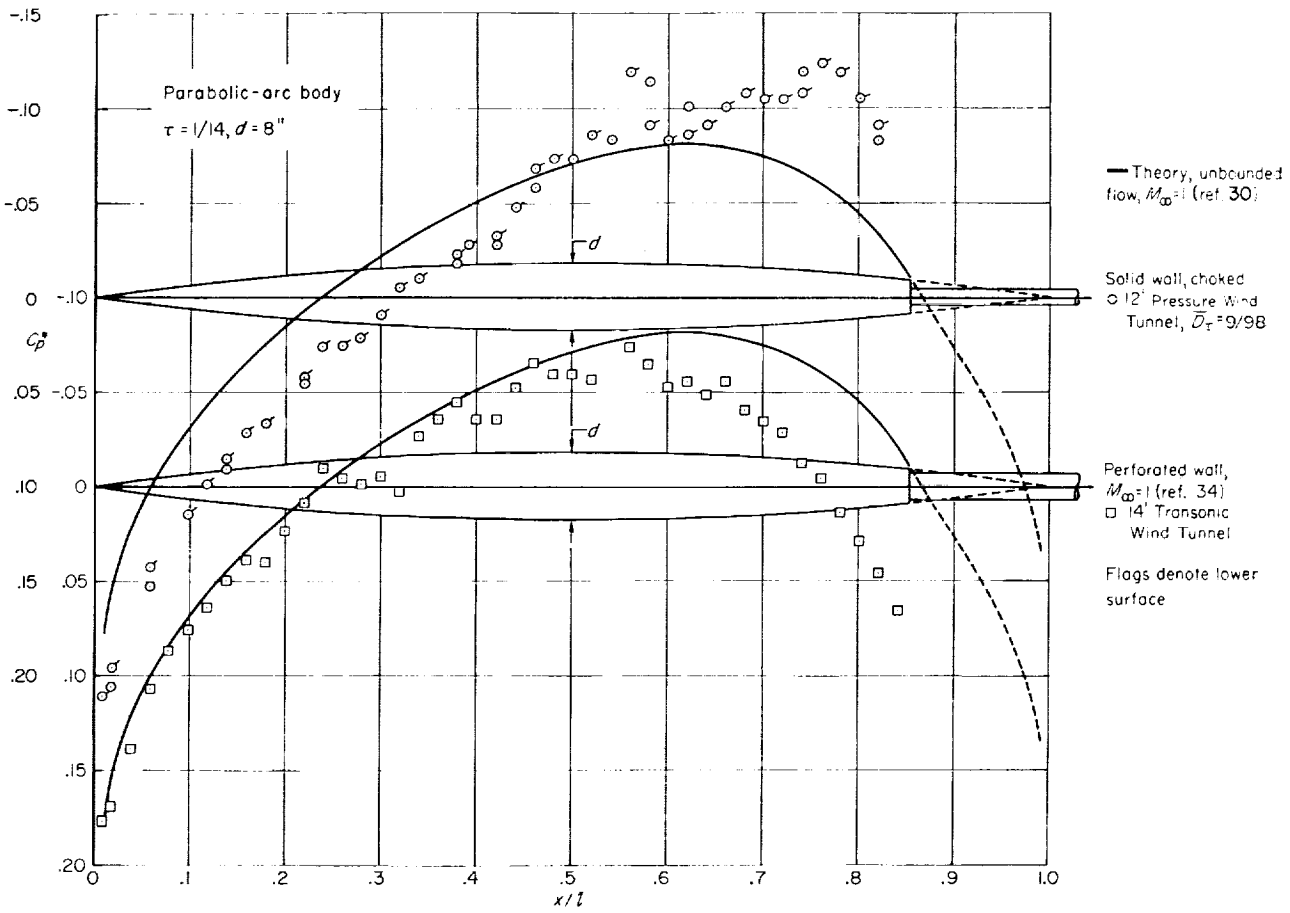

FIGURE 21.—Experimental and theoretical pressure distributions for parabolic-arc bodies of thickness ratio 1/14 and maximum diameter 8 inches.

in the supersonic region. The solid horizontal line represents the position of the wall in the tests of the body of thickness ratio 1/6 in the 12-Foot Pressure Wind Tunnel. This diagram shows that the wind-tunnel walls are sufficiently far away that the results for this particular body should be uninfluenced by interference effects of the wave reflection type. This result appears to be in complete agreement with the observed properties of the results measured in the choked wind tunnel and presented in figure 18. The broken horizontal lines represent the positions of the walls relative to the characteristic network for the tests of the bodies of thickness ratio 1/12 and 1/14. The results for these bodies are obtained from those for the body of thickness ratio 1/6 by application of the transonic similarity rule for axisymmetric flow, which states that the flow fields associated with sonic flow past an affinely related family of slender bodies of revolution can be brought into coincidence by stretching the lateral coordinates in inverse proportion to the thickness ratio. The results are plotted in figure 22 with a distorted lateral scale so that a single characteristic diagram will suffice for all cases. It is evident that the wind-tunnel walls are no longer sufficiently far away to prevent some of the characteristics that reflect from the walls from impinging on the rear of the bodies of thickness ratios 1/12 and 1/14. These results show, moreover, that the most forward reflected characteristic strikes the body at about 55 percent of the body length in the tests of the body of thickness ratio 1/12, about 50 percent of the body length in the tests of the smaller body of thickness ratio 1/14, and about 40 percent of the body length in the tests of the larger body of thickness ratio 1/14. The effect of the reflected characteristics striking the body is to

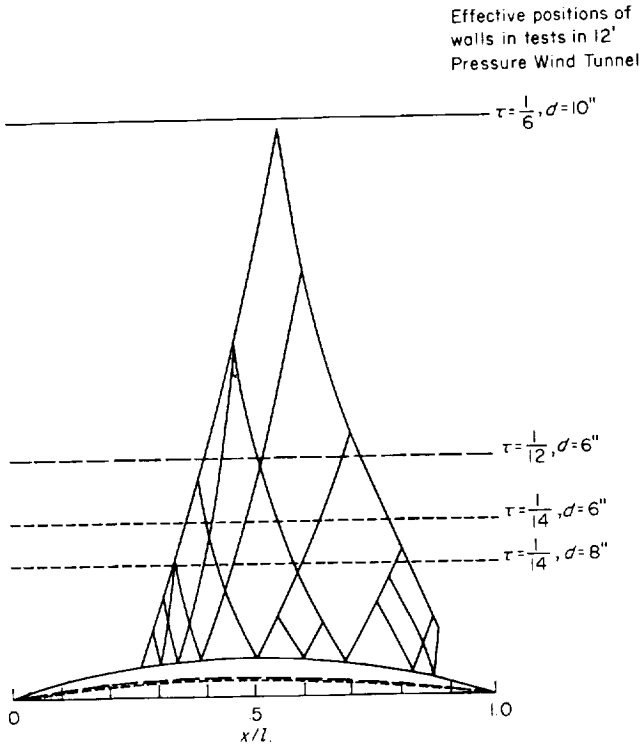

FIGURE 22.—Characteristic diagram for parabolic-arc body of revolution in an unbounded flow with free-stream Mach number 1 (ref. 35) and effective positions of walls in tests in the Ames 12-Foot Pressure Wind Tunnel.

make the pressure coefficients more negative, since the outgoing characteristics represent expansion waves that reflect from the solid wall of the tunnel as expansion waves. Evidence of the absence or presence of such effects is clearly visible in the results of the tests in the choked wind tunnel presented in figures 18 through 21.

Objection might be raised to the argument presented in the preceding paragraph on the basis that the characteristic diagram is not only calculated by means of an approximate theory, but applies to an unbounded flow with free-stream Mach number 1 rather than to a flow in a choked wind tunnel. Although considerable evidence has been given in the preceding discussion showing that the conditions in the vicinity of the body are very similar in these two flows, very little information has been provided regarding the conditions at greater distances from the body. Figure 23 has been prepared, therefore, to provide a comparison of the theoretical and experimental results for the location of the sonic point along the wall of the test section for each of the tests in the 12-Foot Pressure Wind Tunnel. In this figure, the calculated position of the sonic point is indicated by a filled symbol for each of the four bodies, and the corresponding local Mach number distribution measured along the wall of the test section is indicated by a series of similar open symbols. Although the experimental data are rather limited in quantity for each of the bodies, it can be seen that the theoretical and experimental results are in good agreement. This observation serves further to confirm the conclusion that substantial interference effects of the wave reflection type are present in the experimental results obtained in the 12-Foot Pressure Wind Tunnel for the pressures on the rear of the parabolic-arc bodies of thickness ratios 1/12 and 1/14.

It is important to note before leaving the discussion of parabolic-arc bodies that the results

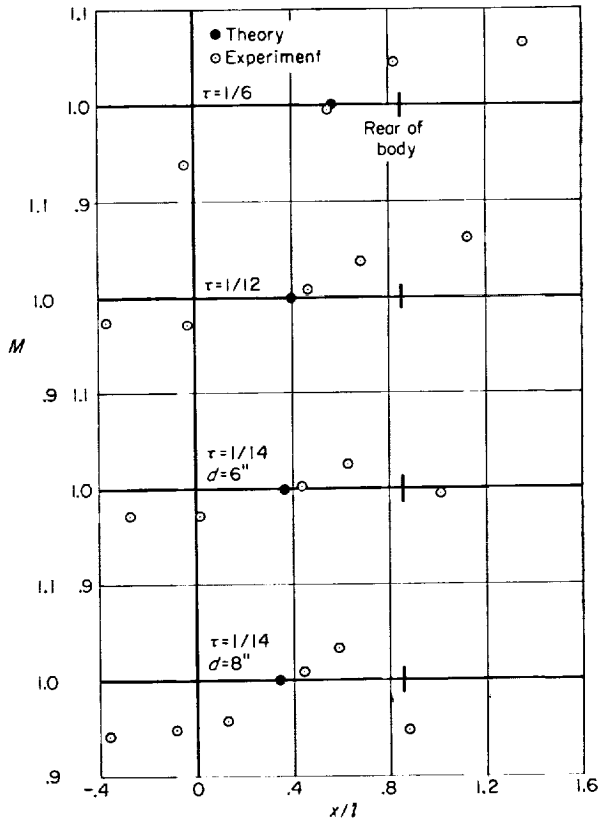

FIGURE 23.—Local Mach number distributions along wall of the test section of the Ames 12-Foot Pressure Wind Tunnel in the tests under choking condition of four different parabolic-arc bodies of revolution.

of the tests in the transonic wind tunnels (figs. 19 through 21) also display unmistakable evidence of the presence of interference effects of the wave reflection type, although of opposite sign, at about the same station on each of the bodies as in the tests in the choked wind tunnels. Although the test section of the 14-Foot Transonic Wind Tunnel is somewhat larger than that of the 12-Foot Pressure Wind Tunnel, it can be seen from figure 23 that the most forward point at which such effects would be expected to be observed is indeed only very slightly farther aft in the transonic wind tunnel than in the choked wind tunnel. The sign of the interference effects in the transonic wind tunnel is not so simple to ascertain theoretically, since the reflections from the solid part of the wall are expansion waves and those from the open part of the wall are compression waves. It appears from the results presented in figures 19 through 21, however, that the influence of the reflections from the partly open wall of the 14–Foot Transonic Wind Tunnel is very nearly equal in magnitude but opposite in sign to that of the reflections from the solid wall of the 12-Foot Pressure Wind Tunnel. This aspect of wind-tunnel wall interference imposes strong restrictions on the maximum length of bodies for which reliable results can be determined in either a transonic wind tunnel with partly open walls or a solid-wall wind tunnel operating in the choked condition. These restrictions become increasingly severe, moreover, as the thickness ratio is diminished, and it is necessary to use models that are not only smaller in diameter but also smaller in length to prevent the reflected waves from impinging on the rear of the model.

Smooth bodies with maximum thickness at 30 and 70 percent of the body length.—It was shown in the preliminary qualitative discussion of interference effects at Mach number 1 that interference effects of the subsonic type observed on the front of a body of given thickness ratio and length tend to increase as the point of maximum thickness is moved rearward along the length of the body; whereas interference effects of the wave reflection type observed on the rear of the body tend to increase as the point of maximum thickness is moved forward. These effects are illustrated by an interesting set of theoretical and experimental results presented in figures 24, 25, and 26. The experimental data refer to the pressure distributions measured in the Ames 12-Foot Pressure Wind Tunnel and in the Ames 14-Foot Transonic Wind Tunnel on a pair of bodies, one of which has the point of maximum thickness located at 70 percent and the other at 30 percent of the body length. Both bodies have a thickness ratio of 1/12 and a maximum diameter of 6 inches. It may be noted that the two bodies have the same thickness ratio and maximum diameter and were tested in the same two wind tunnels as the parabolic-arc body for which results are shown in figure 19. The results shown in figures 19, 24, and 25 are thus directly comparable, and may be considered as a single family to illustrate the effects of the location of the point of maximum thickness.

The ordinates of the surface of the bodies for which experimental data are presented in figures 24, 25, and 26 are given, respectively, by

$$R/l=A[(x/l)-(x/l)^n] \tag{29}$$

and

$$R/l=A[(1-x/l)-(1-x/l)^n] \tag{30}$$

where A is related to the thickness ratio τ and n by

$$A=\frac{n^{n/(n-1)}}{2(n-1)}\tau \tag{31}$$

and n and τ have the values 6.03 and 1/12. Both of the bodies are truncated at the station along the rear where the diameter is half of the maximum diameter in order to permit the model to be mounted on the support. The experimental data from the Ames 14-Foot Transonic Wind Tunnel are taken from reference 37 by McDevitt and Taylor and need no further description here. The data from the Ames 12-Foot Pressure Wind Tunnel were obtained with the wind tunnel operating in the choked condition, and with the same model used in the tests in the transonic wind tunnel. The results for the pressure distributions measured on the surface of each body are shown in figures 24 and 25, and those for the local Mach number distributions measured along the wall of the choked wind tunnel are shown in figure 26. The theoretical pressure distributions shown in figures 24 and 25 are again those indicated for an unbounded flow with free-stream Mach number 1 by the approximate theory of reference 30. The latter results are for a complete body with ordi-

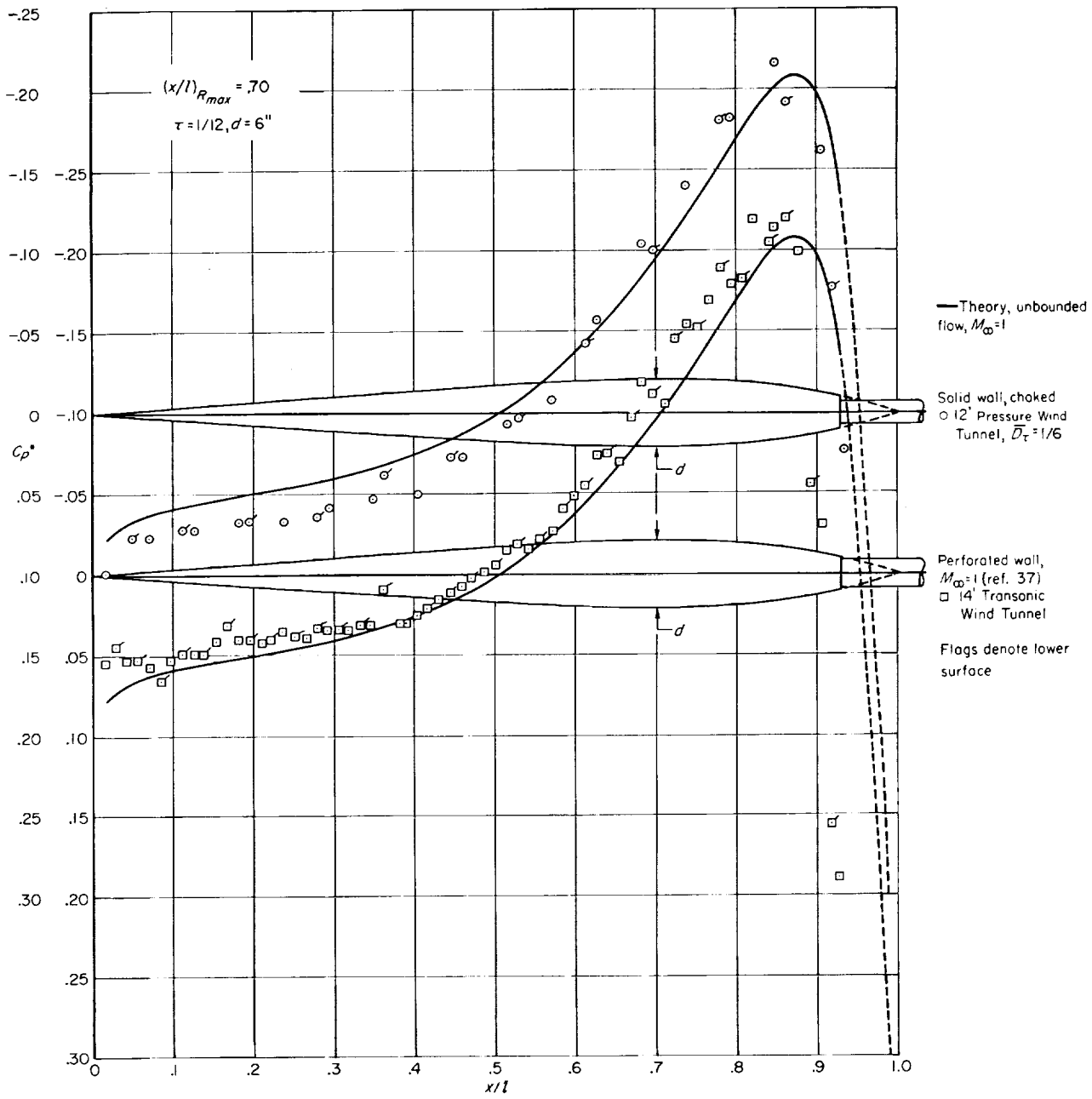

FIGURE 24.— Experimental and theoretical pressure distributions for body of thickness ratio 1/12 with maximum thickness at 70 percent of the body length.

nates very slightly different from those of the wind tunnel models, inasmuch as the exponent 6.03 that appears in equations (29), (30), and (31) has been replaced by 6 to simplify the calculations. The theoretical pressure distributions for these bodies have not been given previously, but have been computed following exactly the same procedures as are described in reference 30 for the parabolic-arc bodies. The resulting values for C_p* along the surface of the bodies are tabulated in table I and are plotted in figures 24 and 25 together with both sets of experimental results.

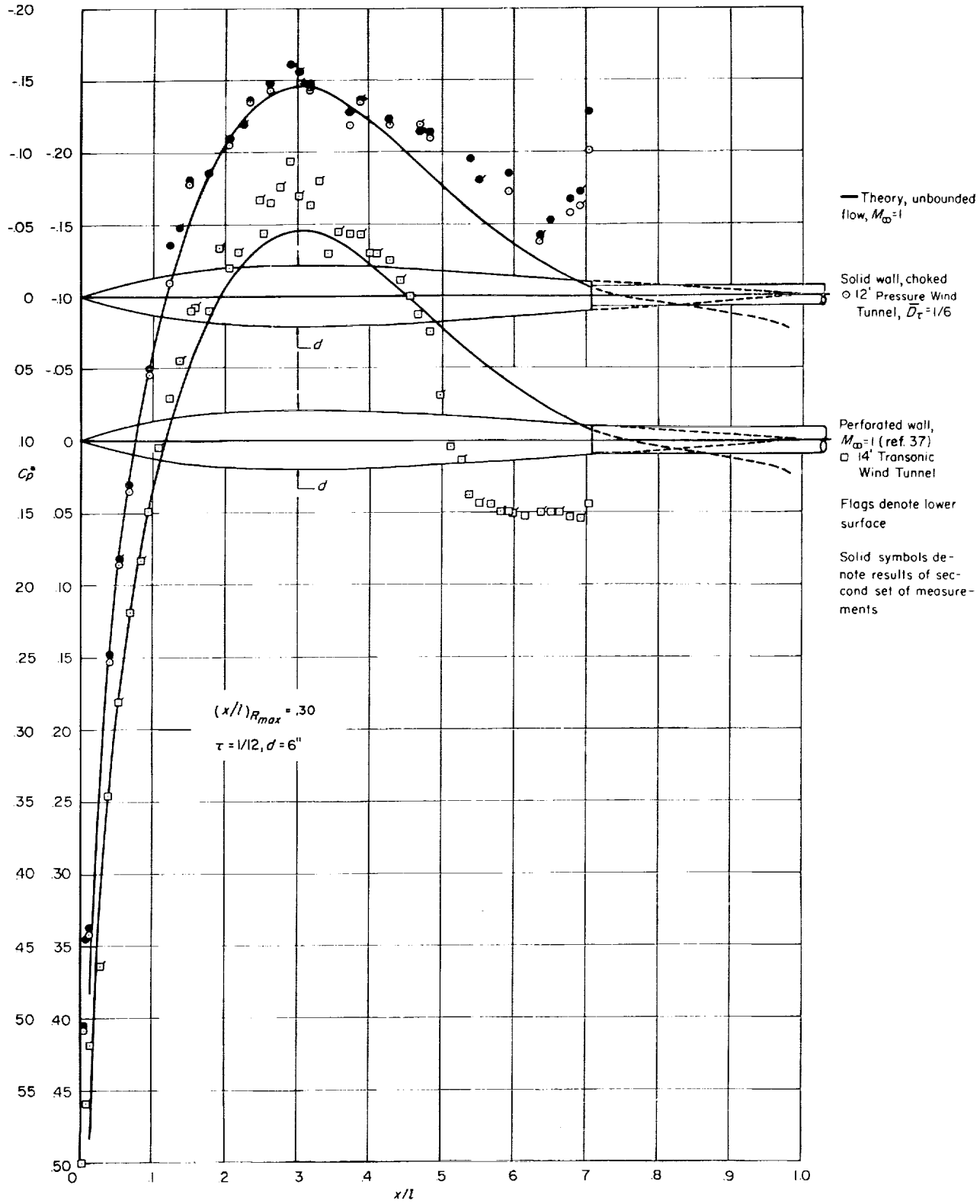

FIGURE 25.—Experimental and theoretical pressure distributions for body of thickness ratio 1/12 with maximum thickness at 30 percent of the body length.

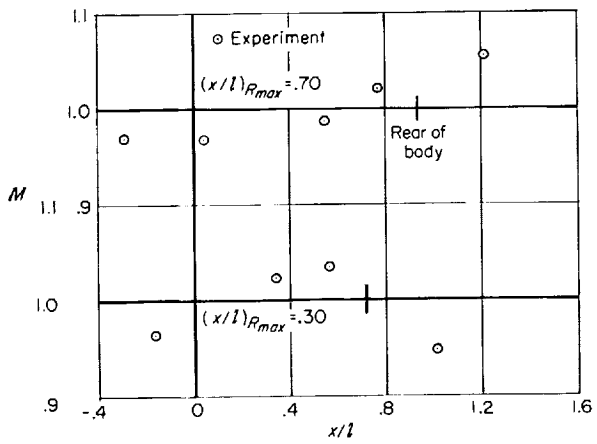

FIGURE 26. Local Mach number distributions along wall of the test section of the Ames 12-foot Pressure Wind Tunnel in the tests under choking condition of the bodies of thickness ratio 1/12 having maximum thickness at 30 and 70 percent of the body length.

Inspection of the results for the body with maximum thickness at 70 percent of its length (fig. 24) reveals that the two sets of experimental data are in essential agreement with each other, and also with the theoretical results for an unbounded flow with free-stream Mach number 1. It is quite clear, however, that the theoretical values for the positive pressure coefficients along the forward part of the body are slightly smaller than those measured in the choked wind tunnel, and slightly greater than those measured in the transonic wind tunnel. Furthermore, these differences are somewhat larger than those present in the corresponding results for the parabolic-arc body shown in figure 19. On the other hand, the differences among the three sets of results are smaller over the rear of the present body than they are over the rear of the parabolic-arc body. Comparison of the results given in figures 26 and 23 show also that the location of the sonic point along the wall of the wind tunnel is somewhat farther aft than in the case of the parabolic-arc body. These observations are consistent with the properties of wind-tunnel interference described briefly at the outset of this section.

Similar inspection of the results for the body having maximum thickness at 30 percent of its length that are presented in figure 25 reveals trends that are quite the opposite of those observed in the results given in figure 24. These trends, however, are still consistent with the properties of wind-tunnel interference described above. It can be seen, in particular, that all of the experimental and theoretical results are in agreement over the forward part of the body, but that substantial differences develop among the various results over the rear of the body. The latter differences are, in fact, the most striking of all those to be seen in the many comparisons of theoretical and experimental results given in this paper. The results from the transonic wind tunnel indicate that the recompression along the rear of the body begins at about the point of maximum thickness, and proceeds gradually in general agreement with the trend indicated by the theoretical pressure distribution, until, at a point well upstream of the base of the model, a region of rapid recompression is encountered. The pressures indicated by the experimental and theoretical results are widely different downstream of this region, and the general appearance of the results strongly suggests that the rapid recompression observed in the experimental pressure distribution is associated with the presence of a shock wave oriented nearly normal to the flow. The results from the choked wind tunnel also indicate that the recompression along the rear of the body begins at about the point of maximum thickness, and proceeds gradually in general agreement with the trend indicated by the theoretical pressure distribution. No region of rapid recompression is observed, however, and the flow continues to decelerate smoothly until nearly sonic velocity is reached whereupon a region of rapid expansion is observed over the remainder of the length of the body. Although the possibility of such a behavior is readily understandable qualitatively in terms of wind-tunnel interference effects of the wave reflection type that would be anticipated to occur when the sonic point on the wall is as far forward as it is indicated to be for this body in figure 26, the magnitude and abruptness of the expansion were so striking that the model was remounted in the wind tunnel at a later date and a second set of measurements were made. The data obtained in both tests are included in this figure, and it is readily apparent that the two sets of results are in essential agreement. The results obtained in the choked wind tunnel and in the transonic wind tunnel are very different over the rear of this particular body, however, and it is highly unlikely that either set of experimental results represents a good approxi-

mation for the pressure distribution on this body in an unbounded flow with free-stream Mach number 1. It is quite possible, on the other hand, that a good approximation is provided once again by the theoretical results, since they agree with the experimental results in regions where interference effects are not expected to be significant and are intermediate between the experimental results obtained in wind tunnels with solid and partly open test sections in the regions where interference effects of opposite sign are expected in the two wind tunnels.

CONCLUDING REMARKS

In summary, two principal conclusions emerge from the foregoing investigation of wind-tunnel interference effects in two-dimensional and axisymmetric flows. The first is that the experimental data support the general result indicated by theory that the flow in the vicinity of the model in a test section having solid walls and operating in the choked condition has a close resemblance to that in an unbounded flow with free-stream Mach number 1, provided the dimensions of the model are sufficiently small compared with those of the test section. It appears, furthermore, that the results obtained in this way are at least as accurate as those obtained in a transonic wind tunnel with partly open test section. The second conclusion is that substantial interference effects, particularly those of the wave-reflection type, may be encountered under certain conditions, both in choked wind tunnels and in transonic wind tunnels, and that the reduction of these interference effects to acceptable limits may require the use of models of unusually small size. A further result of somewhat secondary significance in the present investigation is that the theoretical pressure distributions indicated by transonic flow theory for unbounded flows with free-stream Mach number 1 continue to be of almost surprising accuracy, considering both the small perturbation approximation inherent in the fundamental equations of the theory and the novel nature of some of the procedures used to obtain approximate solutions of these equations.

The results of this investigation for axisymmetric flow are of interest not only because of the frequent use of a body of revolution in aeronautical design, but also because of the central role of the body of revolution in applications of the transonic area and equivalence rules. It should be noted, moreover, that the fundamental property of the flow associated with these rules provides a strong suggestion that conclusions similar to those given in the preceding paragraph would also be found upon investigation of three-dimensional flows without axial symmetry. This possibility, together with the demonstrated existence of interference effects of large magnitude in transonic wind tunnels with partly open walls, should provide ample assurance that the continued investigation of the usefulness of a choked wind tunnel for the simulation of an unbounded flow with free-stream Mach number 1 is a worthwhile task.

AMES RESEARCH CENTER
NATIONAL AERONAUTICS AND SPACE ADMINISTRATION
MOFFETT FIELD, CALIF., *Jan. 20, 1960*

REFERENCES

1. Guderley, K. G.: Theorie schallnaher Strömungen. Springer-Verlag, Berlin, Göttingen, Heidelberg, 1957.
2. Page, William A.: Experimental Study of the Equivalence of Transonic Flow about Slender Cone-Cylinders of Circular and Elliptic Cross Section. NACA TN 4233, 1958.
3. Spreiter, John R.: Aerodynamics of Wings and Bodies at Transonic Speeds. Jour. Aero/Space Sci., vol. 26, no. 8, Aug. 1959, pp. 465–486.
4. Page, William A., and Spreiter, John R.: Some Applications of Transonic-Flow Theory to Problems of Wind-Tunnel Interference. Paper presented to Wind Tunnel and Model Testing Panel of the Advisory Group for Aeronautical Research and Development, Rhode St. Genese, Belgium, March 2–5, 1959.
5. Armstrong, A. H., Holt, M., and Thornhill, C. K.: Transonic Flow Past a Wedge with Detached Shock Wave. Jour. Aero. Sci., vol. 19, no. 10, Oct. 1952, p. 715.
6. Marschner, Bernard W.: The Flow Over a Body in a Choked Wind Tunnel and in a Sonic Free Jet. Jour. Aero. Sci., vol. 23, no. 4, April 1956, pp. 368–376.
7. Guderley, Gottfried: Two-Dimensional Flow Patterns with a Free-Stream Mach Number Close to One. USAF WADC Tech. Rep. 6343, 1951.
8. Barish, David T.: Interim Report on a Study of Mach One Wind Tunnels. USAF WADC Tech. Rep. 52–88, 1952.
9. Spreiter, John R., Alksne, Alberta Y., and Hyett, B. Jeanne: Theoretical Pressure Distributions for Several Related Nonlifting Airfoils at High Subsonic Speeds. NACA TN 4148, 1958.

10. von Kármán, Theodore: The Similarity Law of Transonic Flow. Jour. Math. and Phys., vol. XXVI, no. 3, Oct. 1947, pp. 182–190.
11. Guderley, Gottfried, and Yoshihara, Hideo: The Flow Over a Wedge Profile at Mach Number 1. Jour. Aero. Sci., vol. 17, no. 11, Nov. 1950, pp. 723–735.
12. Morioka, Shigeki: High Subsonic Flow Past a Wedge in a Two-Dimensional Wind Tunnel at its Choked State. Jour. Phys. Soc. Japan, vol. 14, no. 8, Aug. 1959, pp. 1098–1101.
13. Guderley, Gottfried, and Yoshihara, Hideo: Two-Dimensional Unsymmetric Flow Patterns at Mach Number 1. Jour. Aero. Sci., vol. 20, no. 11, Nov. 1953, pp. 757–768.
14. Kusukawa, Ken-Ichi: On the Two-Dimensional Compressible Flow Over a Thin Symmetric Obstacle With Sharp Shoulders Placed in an Unbounded Fluid and in a Choked Wind Tunnel. Jour. Phys. Soc. Japan, vol. 12, no. 9, Sept. 1957, pp. 1031–1041.
15. Helliwell, J. B.: Two-Dimensional Flow at High Subsonic Speeds Past Wedges in Channels with Parallel Walls. Journ. Fluid Mech., vol. 3, pt. 4, Jan. 1958, pp. 385–403.
16. Imai, Isao: Approximation Methods in Compressible Fluid Dynamics. Technical Note BN–95, Inst. for Fluid Dynamics and Appl. Math., Univ. of Maryland, 1957.
17. Cole, Julian D.: Drag of Finite Wedge at High Subsonic Speeds. Jour. Math. and Phys., vol. 30, no. 2, July 1951, pp. 79–93.
18. Weinstein, A.: Transonic Flow and Generalized Axially Symmetric Potential Theory. NOLR 1132, Naval Ordnance Lab., White Oak, Silver Spring, Maryland, 1950, pp. 73–82.
19. Diaz, J. B.: Two-Dimensional Flow at High Subsonic Speeds Past Wedges in Channels with Parallel Walls. Jour. Math. and Phys., vol. XXXVIII, no. 1, April 1959, pp. 75–76.
20. Guderley, Gottfried: The Wall Pressure Distribution in a Choked Tunnel. USAF WADC Tech. Rep. 53–509, Dec. 1953.
21. Nelson, William J., and Bloetscher, Frederick: An Experimental Investigation of the Zero-Lift Pressure Distribution Over a Wedge Airfoil in Closed, Slotted, and Open-Throat Tunnels at Transonic Mach Numbers. NACA RM L52C18, 1952.
22. Knechtel, Earl D.: Experimental Investigation at Transonic Speeds of Pressure Distributions Over Wedge and Circular-Arc Airfoil Sections and Evaluation of Perforated-Wall Interference. NASA TN D–15, 1959.
23. Spreiter, John R., and Alksne, Alberta Y.: Thin Airfoil Theory Based on Approximate Solution of the Transonic Flow Equation. NACA Rep. 1359, 1958. (Supersedes NACA TN 3970)
24. Nocilla, Silvio: Campi di moto transonici attorno a profili alari: applicazioni. Atti della Accademia delle Scienze de Torino, v. 90, 1955–56, pp. 311–331.
25. Tomotika, S., and Tamada, K.: Studies on Two-Dimensional Transonic Flows of Compressible Fluid. Part III. Quart. Appl. Math., vol. IX, no. 2, July 1951, pp. 129–147.
26. Larson, P. O., and Sörensén, H.: Bestämning av Tryckfördelningen på en två-Dimensionell Vinge vid Olika Blockeringsmachtal. Flygtekniska Försökanstalten Rapport SE–52, Stockholm, Sweden.
27. Oswatitsch, K., and Berndt, S. B.: Aerodynamic Similarity at Axisymmetric Transonic Flow Around Slender Bodies. KTH Aero TN 15, Royal Inst. Tech., Stockholm, Sweden, 1950.
28. Guderley, Gottfried: Axial-Symmetric Flow Patterns at a Free-Stream Mach Number Close to One. USAF Tech. Rep. 6285, 1950.
29. Spreiter, John R., and Alksne, Alberta Y.: Aerodynamics of Wings and Bodies at Mach Number One. Proc. ASME Third U.S. Natl. Cong. Appl. Mech., 1958.
30. Spreiter, John R., and Alksne, Alberta Y.: Slender-Body Theory Based on Approximate Solution of the Transonic Flow Equation. NASA Rep. 2, 1959.
31. Yoshihara, Hideo: On the Flow Over a Cone-Cylinder Body at Mach Number One. USAF WADC Tech. Rep. 52–295, Nov. 1952.
32. Berndt, Sune B.: Theoretical Aspects of the Calibration of Transonic Test Sections. ZAMP, vol. IXb, Fasc. 5/6 Sonderband, 1958, pp. 105–124.
33. Drougge, Georg: An Experimental Investigation of the Interference Between Bodies of Revolution at Transonic Speeds with Special Reference to the Sonic and Supersonic Area Rules. The Aeronautical Research Institute of Sweden, Meddelande 83, FFA Rep. 83, Stockholm, 1959.
34. Taylor, Robert A., and McDevitt, John B.: Pressure Distributions at Transonic Speeds for Parabolic-Arc Bodies of Revolution Having Fineness Ratios of 10, 12, and 14. NACA TN 4234, 1958.
35. Oswatitsch, K.: Die Berechnung wirbelfreier achsensymmetrischer Überschallfelder. Österreichisches Ingenieur-Archiv, Band X, Heft 4, 1956, pp. 359–382.
36. Oswatitsch, K., and Keune, F.: The Flow Around Bodies of Revolution at Mach Number 1. Proc. Conf. on High-Speed Aeronautics, Polytechnic Institute of Brooklyn, Brooklyn, N.Y., Jan. 20–22, 1955, pp. 113–131.
37. McDevitt, John B., and Taylor, Robert A.: Pressure Distributions at Transonic Speeds for Slender Bodies Having Various Axial Locations of Maximum Diameter. NACA TN 4280, 1958.

TABLE I.– CALCULATED PRESSURE DISTRIBUTION FOR BODIES OF THICKNESS RATIO 1/12 WITH MAXIMUM THICKNESS AT 30 AND 70 PERCENT OF THE BODY LENGTH

(a) $(x/l)_{R_{max}}=0.70$

x/l	C_p*	x/l	C_p*
Parabolic		0.6773085	−0.081400
		.6973085	−.094422
0.0173085	0.077898	.7173085	−.108154
.0373085	.069784	.7373085	−.122544
.0573085	.065270	.7573085	−.137425
.0773085	.062034	.7773085	−.152642
.0973085	.059465	.7973085	−.167848
.1173085	.057267	.8173085	−.182658
.1373085	.055313	.8373085	−.196485
.1573085	.053490		
.1773085	.051755	Hyperbolic	
.1973085	.050037		
.2173085	.048316	0.8373085	−0.196485
.2373085	.046534	.8473085	−.201940
.2573085	.044675	.8573085	−.206067
.2773085	.042688	.8673085	−.208455
.2973085	.040548	.8773085	−.208568
.3173085	.038210	.8873085	−.205703
.3373085	.035647	.8973085	−.198917
.3573085	.032806	.9073085	−.186908
.3773085	.029665	.9173085	−.167791
.3973085	.026165	.9273085	−.138591
.4173085	.022277	.9373085	−.093257
.4373085	.017956		
.4573085	.013158	Elliptic	
.4773085	.007844		
.4973085	.001972	0.9400	−0.0766
.5173085	−.004491	.941932	−.060891
.5373085	−.011588	.9500	−.0055
.5573085	−.019345	.9600	.0618
.5773085	−.027815	.9700	.1351
.5973085	−.037004	.9800	.2240
.6173085	−.046930	.9900	.3610
.6373085	−.057658		
.6573085	−.069127		

(b) $(x/l)_{R_{max}}=0.30$

x/l	C_p*	x/l	C_p*
Parabolic		0.3836582	−0.129541
		.4036582	−.121825
0.0036582	0.834674	.4236582	−.113400
.0136582	.484435	.4436582	−.104448
.0236582	.360727	.4636582	−.095274
.0336582	.282695	.4836582	−.085997
.0436582	.225524	.5036582	−.076852
.0536582	.179877	.5236582	−.067892
.0636582	.141966	.5436582	−.059293
.0736582	.109431	.5636582	−.051054
.0836582	.080835	.5836582	−.043302
.0936582	.055425	.6036582	−.035993
.1036582	.032590	.6236582	−.029212
.1136582	.011877	.6436582	−.022883
.1236582	−.006872	.6636582	−.017062
.1336582	−.023914	.6836582	−.011638
.1436582	−.039664	.7036582	−.006603
.1536582	−.053677		
.1636582	−.066727	Elliptic	
.1736582	−.078340		
.1836582	−.088950	0.7136582	−0.004470
.1936582	−.098431	.7236582	−.003048
.2036582	−.106928	.7336582	−.001761
.2136582	−.114470	.7436582	−.000576
.2236582	−.121116	.7536582	.000476
.2336582	−.126931	.7636582	.001548
.2436582	−.131958	.7736582	.002485
.2536582	−.136271	.7836582	.003447
.2636582	−.139914	.8036582	.005173
		.8236582	.006777
Hyperbolic		.8436582	.008308
		.8636582	.009810
0.2636582	−0.139914	.8836582	.011335
.2836582	−.144579	.9036582	.012940
.3036582	−.146046	.9236582	.014714
.3236582	−.144829	.9436582	.016805
.3436582	−.141398	.9636582	.019554
.3636582	−.136177	.9836582	.024215

U.S. GOVERNMENT PRINTING OFFICE: 1960